MICROTRAC
PARTICLE CHARACTERIZATION

APPLICATION BOOKLET

CARBON NEUTRALITY

part of VERDER

CONTENTS

04 CO_2 breakthrough curve measurement using BELCAT II

06 Breakthrough curve measurement for binary gas mixtures (CO_2 and water vapor) by MS-5A packed bed in BELCATII

10 Adsorption and Recovery of CO_2 in Air Using Metal Organic Frameworks (CALF-20) Assuming DAC Condition

15 Investigation of CO_2 adsorption and recovery between ambient and high temperature

18 Reproducibility and effective adsorption loading amount evaluation of high-pressure CO_2 adsorption isotherm of activated carbon (@25 °C, 120 °C)

21 Pore Structure Analysis of Cement Hardened Body

23 Micro-pore Evaluation of Mesoporous Y-Type Zeolites by CY-method from Ar and N_2 adsorption isotherms

25 Investigation of cylidrical porous materials (zeolite and mesoporous silica) by NLDFT and GCMC
-Optimum adsorbate and theory

29 Increased accuracy in the pore structure analysis of activated carbons using a new GCMC kernel based on a slit-pore model with carbon surface heterogeneity

31 Porous Metal Coordination Polymer (MOF/PCP) Materials
-Specific surface area and pore structure analysis-

39 Repeated performance evaluation of water vapor adsorption and desorption for PCP/MOF (porous metal organic framework)

MICROTRAC SOLUTIONS FOR CARBON NEUTRALITY

MICROTRAC offers solutions for research, development, and quality control in the field of adsorbent, catalyst evaluation to help realize a decarbonized and carbon neutral society.

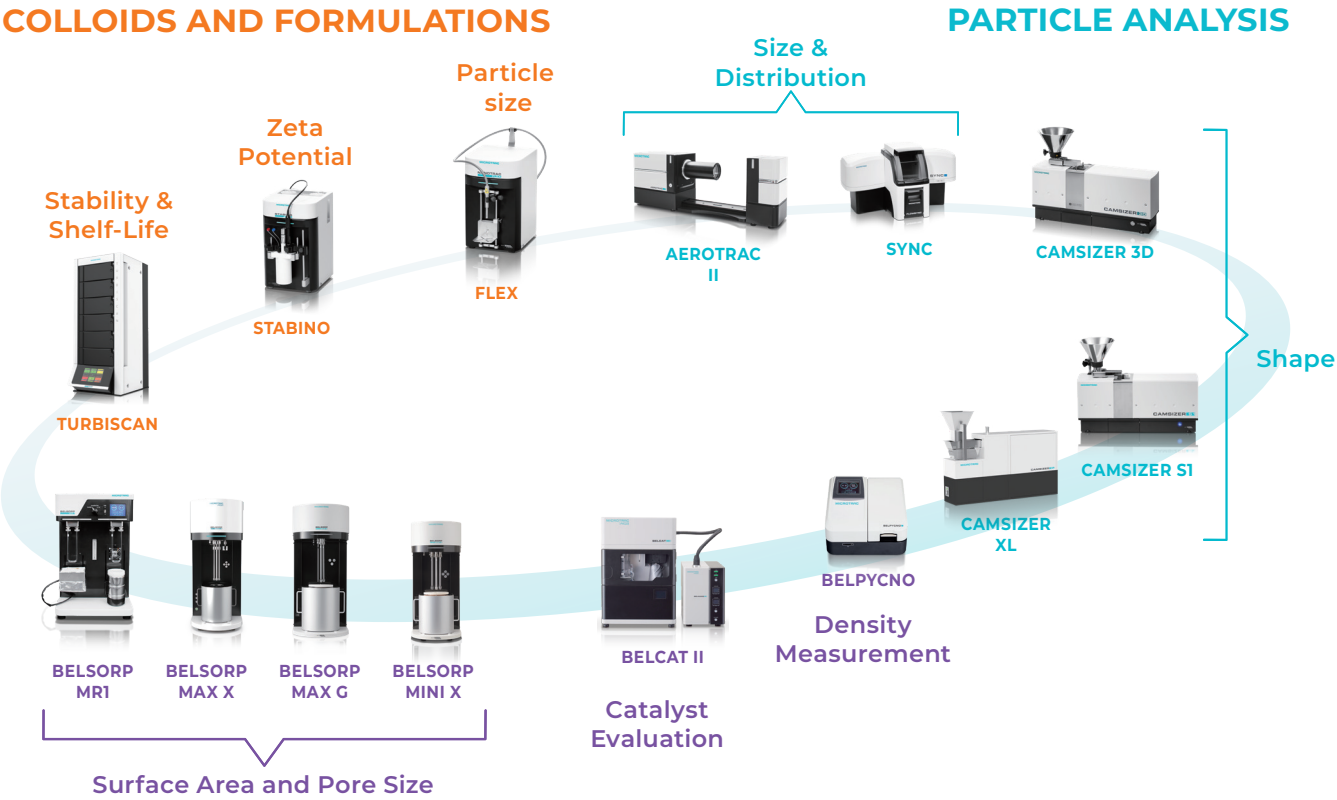

1. CCUS: EVALUATION OF MATERIALS FOR EFFECTIVE UTILIZATION, SEPARATION, AND RECOVERY OF CO_2

1. **Evaluation of specific surface area, pore size distribution, and adsorbed amount for CO_2 adsorbent zeolite, PCP/MOF)**
    - Gas/vapor adsorption measurement system; **BELSORP MAX series/BELSORP MINIX**
2. **Evaluation of adsorption and desorption processes for separation performance evaluation (adsorption breakthrough curve measurement) of mixed gases such as CO_2/H_2O**
    - Catalyst evaluation system; **BELCAT II**

2. CCU: MATERIAL EVALUATION FOR CATALYST, CEMENT, AND CONCRETE FIELDS FOR EFFECTIVE UTILIZATION OF CO_2 EMISSIONS

- Catalyst evaluation system; **BELCAT II + BELMASS II**
- True density measuring syste; **BELPYCNO**
- Mercury porosimeter; **BELPORE**
- Particle size distribution analyzer; **SYNC/ NANOTRAC WAVE II**
- Slurry dispersion and stability evaluation; **STABINO ZETA/ TURBISCAN series**

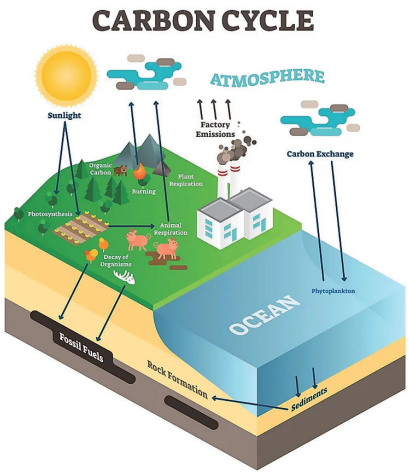

CO_2 BREAKTHROUGH CURVE MEASUREMENT USING BELCAT II

1. INTRODUCTION

The Adsorption breakthrough curve (BTC) measurement is widely used as an assay method to examine design parameters and adsorption rates for adsorption process. In this article, aiming at single component gas recovery of CO_2, which is one of the greenhouse gases. we conducted CO_2 breakthrough curve measurement, and at the same time, helium purge and TPD measurement to observe the regeneration treatment process.

2. EXPERIMENTAL

As an adsorbent, zeolite molecular sieve 5A (amount: 0.1g, particle size: 250 to 500 μm) was packed in a triple structure sample tube for **BELCAT II,** pretreated at 400 °C in helium flow, and a breakthrough curve measurement was carried out in 1% - CO_2/He (50 SCCM) gas flow. After this, the sample tube was purged with helium as a desorption process, and TPD-measurement (temperature programmed desorption) was performed. The same measurement was performed for an empty sample cell. The adsorption/desorption amount in each process and the mass balance in the entire measurement were evaluated from the difference of each profile. The built-in thermal conductivity detector (TCD) was used as a detector.

Pretreatment:	In 100% He flow (50 SCCM) At 400 °C, for 60 minutes.
BTC measurement:	In 1% CO_2/He (50 SCCM) flow, at 25 °C, for 25 minutes.
He purges:	In 100% He (50 SCCM) flow, at 25 °C, for 50 minutes.
TPD measurement:	In 100% He (50 SCCM) flow, at a 10 °C min-1 ramp rate from 25 °C to 200 °C.

3. RESULT AND DISCUSSION

The continuous breakthrough curve – TPD measurement result are shown in Figure 1. The break point and the end point were observed about 5 minutes, and 10 minutes respectively from starting point of the breakthrough curve measurement. On the other hand, it took 50 minutes for the reactivation process, and about 10% of CO_2 was desorbed during the TPD measurement. It is considered that there might be some strong adsorption sites on MS-5A, on which CO_2 molecules can be adsorbed strongly.

Fig. 2 shows the difference between a blank sample measurement and a sample measurement result. From the shaded area of each peak, the adsorption/desorption amount can be calculated (Table 1).

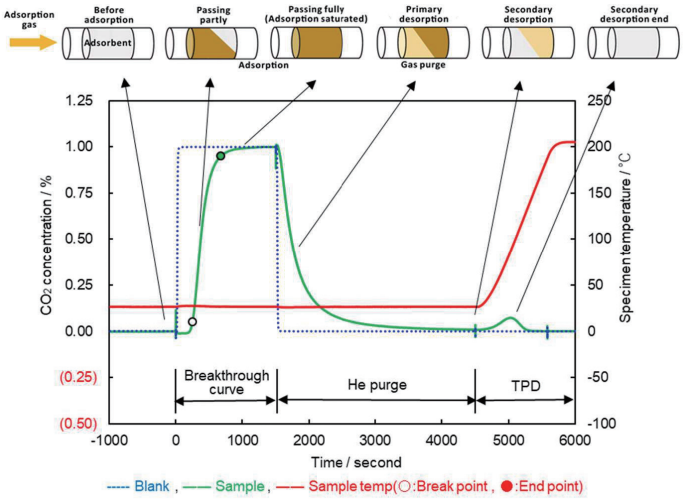

Fig.1 CO_2 breakthrough curve-He purge & TPD measurement of zeolite MS-5A

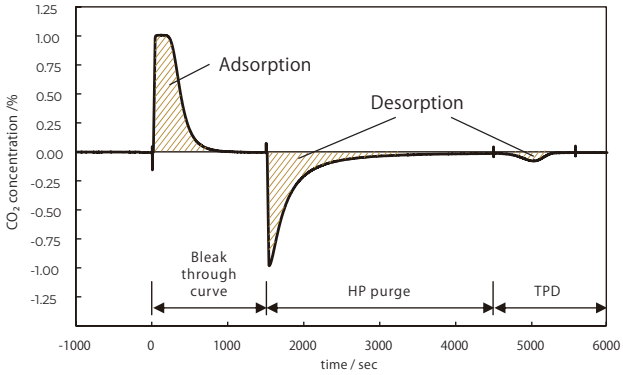

Fig.2 Difference between blank and sample measurement

Table 1 Amount of adsorption and desorption in each process

Breakthrough curve (Ads.)	He purge (Des.)	TPD (Des.)
Ads.amount: 1.41 mmol/g	Des.amount: 1.26 mmol	Des.amount: 0.12 mmol/g
Break point (Saturation degree 5%) : 250 seconds		Peak top tamp.: 90 °C
End point (Saturation degree 95%) : 680 seconds		

Mass balance : (1.26+0.12) / 1.41×100 = 97.9%

Thus, by the continuous breakthrough – He purge – TPD measurement, the adsorption amount and desorption amount (reactivation process) of adsorbents can be evaluated quantitively.

EQUIPMENT

Catalyst Analyzer

BELCAT II

Measurement items

- Thermal desorption spectroscopy
- Adsorption breakthrough curve measurement

BREAKTHROUGH CURVE MEASUREMENT FOR BINARY GAS MIXTURES (CO_2 AND WATER VAPOR) BY MS-5A PACKED BED IN BELCAT II

1. INTRODUCTION

Water vapor is present as a raw material or byproduct in many physical and chemical processes, and when using adsorption process, it is well-known that the adsorption performance of the material changes depending on the presence or absence of water vapor. This is due to the competitive adsorption of each component into the adsorbent, and by evaluating adsorbents under the coexistence of multiple components, it is possible to evaluate their performance closer to practical conditions. This application note introduces an example of evaluation using the **BELCAT II** (MICROTRAC) to measure the adsorption breakthrough curve of CO_2 in the presence of low and high concentrations of water vapor and using CO_2 and humidity probes as detectors.

2. EXPERIMENT

After pretreatment of the adsorbent (Zeolite MS-5A), the adsorption/desorption curve measurement of CO_2 was performed, and the physisorbed amount was desorbed by N_2 purging at room temperature (desorption), and the chemisorbed amount was desorbed by TPD measurement (Temperature Programmed Desorption). The same measurements were also performed in a blank sample tube, and the differences in the waveforms output were used to confirm the amount adsorbed and desorbed in each process and the material balance in the entire measurement. To quantify both CO_2 and H_2O components simultaneously, the CO_2 and humidity sensor output values were used. Fig.1 shows flow path diagram and image of **BELCAT II**.

[Test measurement 1: Low concentration CO_2]

Zeolite molecular sieve 5A (MS-5A, weight: 0.1 g, particle size: 250 to 500 μm) was packed in a triple sample tube and adsorption/desorption measurements were performed under the following conditions.

(1). Pre-treatment:

Under 100%-N_2 (50 SCCM) flow, temperature is raised to 400 °C at 20 °C / min, held for 60 min, and then cooled to 25 °C.

(2). Adsorption breakthrough curve:

Adsorption gas of the following composition (total flow rate of 50 SCCM) was introduced at 25 °C for 100 min (6000 s).

- Single component measurement: 1000 ppm-CO_2 and N_2 balance
- Two-component measurement: 1000 ppm-CO_2, 8000 ppm-H_2O and N_2 balance

(3). Desorption by N_2 purge:

100% N_2 (50 SCCM) at 25 °C for 50 minutes

(4). Desorption by TPD:

Temperature increases from 25 °C to 400 °C at 10 °C / minute and hold for 20 minutes under 100%- N_2 (50 SCCM) flow

[**Test measurement 2: High concentration CO_2**]
Zeolite molecular sieve 5A (MS-5A, weight: 3 g, particle size: 250 to 500 μm) was packed in a triple sample tube and adsorption/desorption measurements were performed under the following conditions.

(1). Pre-treatment:
Under 100%-N_2 (50 SCCM) flow, temperature is raised to 400 °C at 20 °C/min, held for 60 min, and then cooled to 25 °C.

(2). Adsorption breakthrough curve:
Adsorption gas of the following composition (total flow rate of 50 SCCM) was introduced at 50 °C for 300 min (18,000 s).
- Two-component measurement: 14%-CO_2, 7%-H_2O and N_2 balance

(3). Desorption by N_2 purge:
100% N_2 (50 SCCM) at 50 °C for 300 minutes

(4). Desorption by TPD:
Temperature was increased from 50°C to 400°C at 1°C/minute and held for 60 minutes under 100%- N_2 (50 SCCM) flow

Image shows a triple tube for BELCAT II filled with 1 g of adsorbent

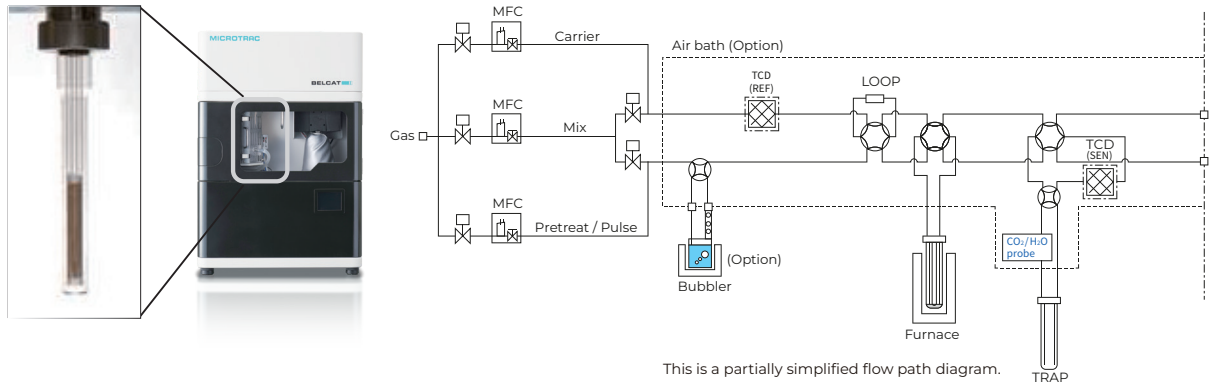

Fig.1 Flow path diagram and image of BELCAT II

3. RESULT & DISCUSSION

Fig. 2 shows the comparative results of adsorption breakthrough measurement and desorption measurement (purging and increasing temperature) of 1,000 ppm single component CO_2 and two-component CO_2 in the presence of water vapor as an example of low-concentration CO_2 evaluation.

In the two-component measurement, CO_2 reaches the breakthrough and endpoints earlier than H_2O. This indicates that MS-5A can adsorb more H_2O than CO_2 under these conditions. As shown in Table 1, the amount of CO_2 adsorbed in the two-component measurement is lower than the amount of CO_2 adsorbed in the single component, so it can be said that the adsorption capacity of CO_2 decreases in the presence of H_2O. Furthermore, the CO_2 concentration ratio is also higher than single component run between 5,000 and 8,000 s, which suggests that the CO_2 adsorbed on the sample was desorbed by substitution of H_2O in the breakthrough curve measurement of the two-component measurement. It can also be confirmed that during desorption, H_2O is not easily desorbed by N_2 purging, and it is desorbed completely during TPD process.

The fact that the mass balance was almost completely obtained in the adsorption and desorption processes indicates the authenticity of this measurement. Thus, by combining **BELCAT II** with CO_2 and H_2O sensors to measure adsorption-breakthrough curves and desorption, it is possible to study the adsorption behavior of not only a single component but also selectively study the adsorption behavior of individual components in multi-component mixtures.

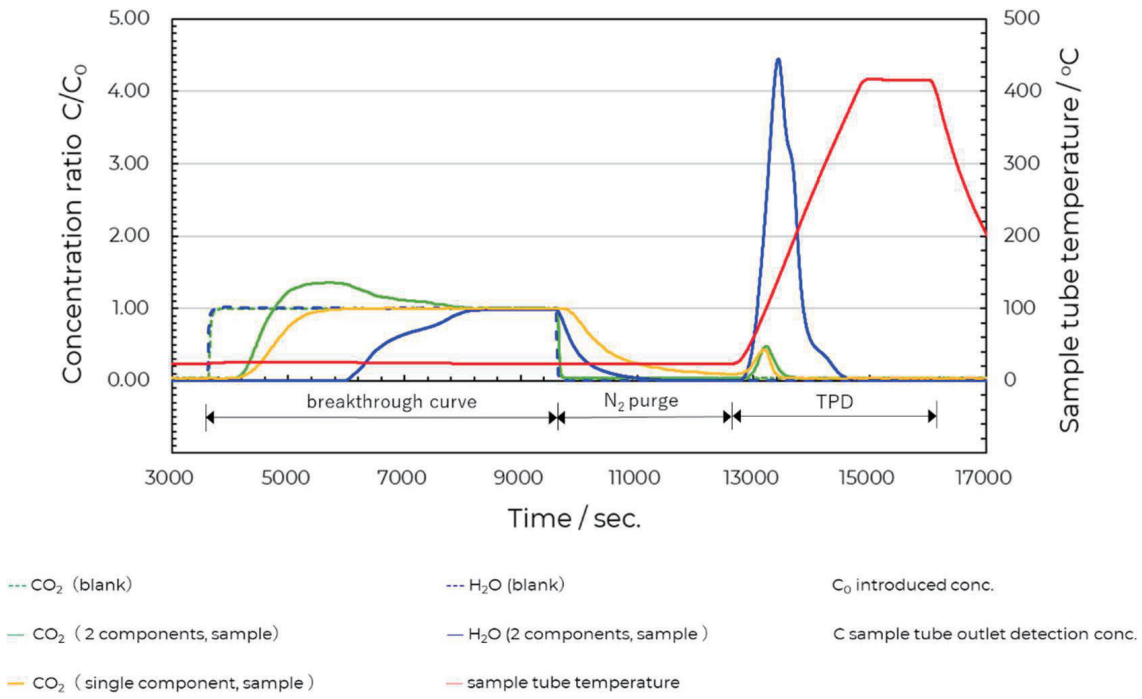

Fig.2 Comparison of adsorption and desorption behavior between CO_2 (1000 ppm) with and without of water vapor including processes of adsorption breakthroug curve, N_2 purging and TPD

Table 1 Adsorption and desorption amount of CO_2 single component and CO_2/H_2O binary component gas mixtures (mmol/g)

	B.T (Ads.)	B.T (Des.)	N_2 purge (Des.)	TPD (Des.)
single-CO_2	0.42	-	0.35	0.06
binary-CO_2	0.31	0.24	0.00	0.06
binary-H_2O	9.8	-	1.2	7.9

Fig. 3 shows the results of adsorption breakthrough measurement of relatively high concentrations of 14% CO_2 and 7% H_2O, assuming gas mixtures from factory exhausts. Under these conditions, the concentrations of CO_2 and H_2O are approximately 140 times and 9 times higher, respectively, than in Fig. 2, indicating that CO_2 is more concentrated than H_2O. Table 2 shows that MS-5A can adsorb more H_2O than CO_2 even under these conditions. Furthermore, the CO_2 concentration ratio is higher than 1 between about 3,000 and 15,000 s. In the breakthrough curve measurement of the two components of CO_2 and H_2O, the amount of CO_2 adsorbed on the sample and then desorbed by its replacement with H_2O can be confirmed to be the same as the results in Fig. 2.

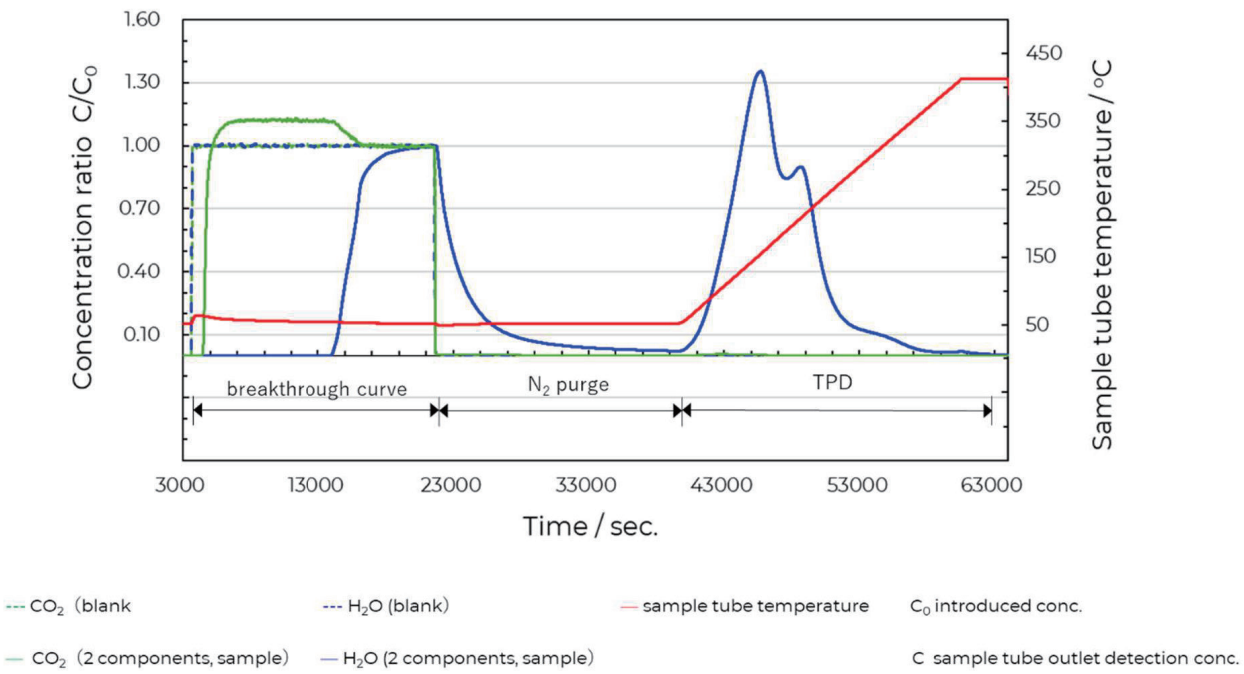

Fig.3 Adsorption and desorption behavior of CO_2 (14%) and H_2O (7%) gas mixture through the processes of adsorption breakthrough curve, N_2 purging and TPD

Table 2 Adsorption and desorption amount of CO_2 and H_2O binary gas mixtures (mmol/g)

	B.T (Ads.)	B.T (Des.)	N_2 purge (Des.)	TPD (Des.)
binary-CO_2	1.8	1.9	0.1	0.1
binary-H_2O	10.4	-	2.2	7.4

4. SUMMARY

These results indicate that the BELCAT II can be used in combination with CO_2 and H_2O sensors to evaluate and study the adsorption and desorption behavior of carbon dioxide, including the adsorption/breakthrough curve evaluation, for single-component CO_2, two-component CO_2, and H_2O, with the aim of finding solutions for a carbon neutral future.

EQUIPMENT

Catalyst Analyzer

BELCAT II

Measurement items

- Thermal desorption spectroscopy
- Adsorption breakthrough curve measurement

ADSORPTION AND RECOVERY OF CO_2 IN AIR USING METAL ORGANIC FRAMEWORKS (CALF-20) ASSUMING DAC CONDITION

1. OVERVIEW

To achieve carbon neutrality by the year 2050, increasing attention is being directed toward Direct Air Capture (DAC) technology, which directly adsorbs, enriches, and recovers approximately 400 ppm of CO_2 from the atmosphere. Since the air contains not only CO_2 but also N_2, O_2, and water vapor, it is essential to evaluate adsorbents under multicomponent conditions. This article introduces the results of a performance evaluation of an adsorbent using the BELCAT II (catalyst analyzer). A column packed with CALF-20 (Zinc-based Calgary Framework 20), a type of metal-organic framework (MOF), was employed for the study. CO_2 was supplied at room temperature under ambient pressure with coexisting N_2, O_2, and H_2O conditions for adsorption breakthrough measurements (separation). The system was then heated to 110 °C while maintaining the composition of the supplied gas to measure CO_2 desorption. These adsorption-desorption cycles were repeated to evaluate the adsorbent's performance.

2. EXPERIMENT

To evaluate the performance of the adsorbent, we conducted the following two experiments. Using the **BELSORP MAX X** (a high-precision gas and vapor adsorption analyzer), we assessed the single-component adsorption isotherms of the metal-organic framework CALF-20 1 at (a) room temperature (25 °C) and (b) high temperature (110 °C), under vacuum conditions up to 100 kPa. The concentrations of each component in the air were assumed to be N_2: 77.4%, CO_2: 400 ppm, and H_2O: 40% RH (at room temperature). We calculated the maximum recoverable amount from the respective isotherms for adsorption at 25 °C and regeneration at 110 °C.

Investigation of single component adsorption amounts for N_2, CO_2, and H_2O

Sample	CALF-20 (measured weight: 0.050 g)
Pre-treatment	Under vacuum, 110 °C, 12 hours
Adsorption Gases	N_2, CO_2, H_2O
Adsorption Temperatures	25 °C (water bath + circulator), 110 °C (heater)

Using the **BELCAT II** (catalyst analyzer), we supplied a multicomponent gas mixture composed of 400 ppm CO_2, 21% O_2, 1.24% H_2O (RH 40% at 25 °C), and 77.4% N_2 at a flow rate of 50 SCCM to a column filled with 1g of the CALF-20 sample at 25 °C and conducted adsorption breakthrough curve measurements (Fig. 1). Following the adsorption measurements, we performed temperature-programmed desorption (TPD) measurements continuously without altering the composition of the supplied gas. These adsorption and desorption measurements were considered one cycle, and were repeated for a total of three cycles. Additionally, we conducted similar measurements using an empty sample tube as a reference and calculated the adsorption and desorption amounts for each process from the differences in concentration changes. To quantify CO_2 in the presence of water vapor, we used a non-dispersive infrared CO_2 probe and an H_2O probe as detectors.

Evaluation of multicomponent adsorption breakthrough and temperature-programmed desorption

Sample	CAF-20 (sample weight: 1.00 g)
Pre-treatment	Under a flow of 100% N_2 (50 SCCM), heated to 110 °C at a rate of 10 °C/min, held for 300 minutes, then cooled to 25 °C
Supplied Gases	Multicomponent gas: 400 ppm CO_2, 21% O_2, 1.24% H_2O (RH 40% at 25 °C), approximately 77% N_2 (50 SCCM)
Adsorption breakthrough curve	Supplied gas flowed at 25 °C for 75 minutes
Temperature programmed desorption	Under the flow of supplied gas, heated from 25 °C to 110 °C at a rate of 2 °C/min, held for 30 minutes
Equipment	BELCAT II (CO_2 probe, H_2O probe)

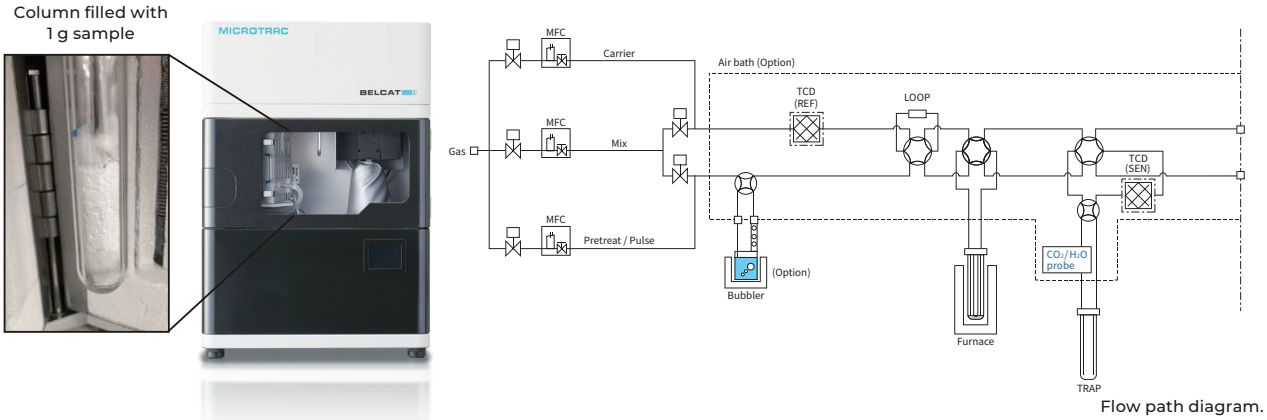

Fig.1 Column image and flow path diagram for adsorption and desorption measurement by BELCAT II

3. RESULT & DISCUSSIONS

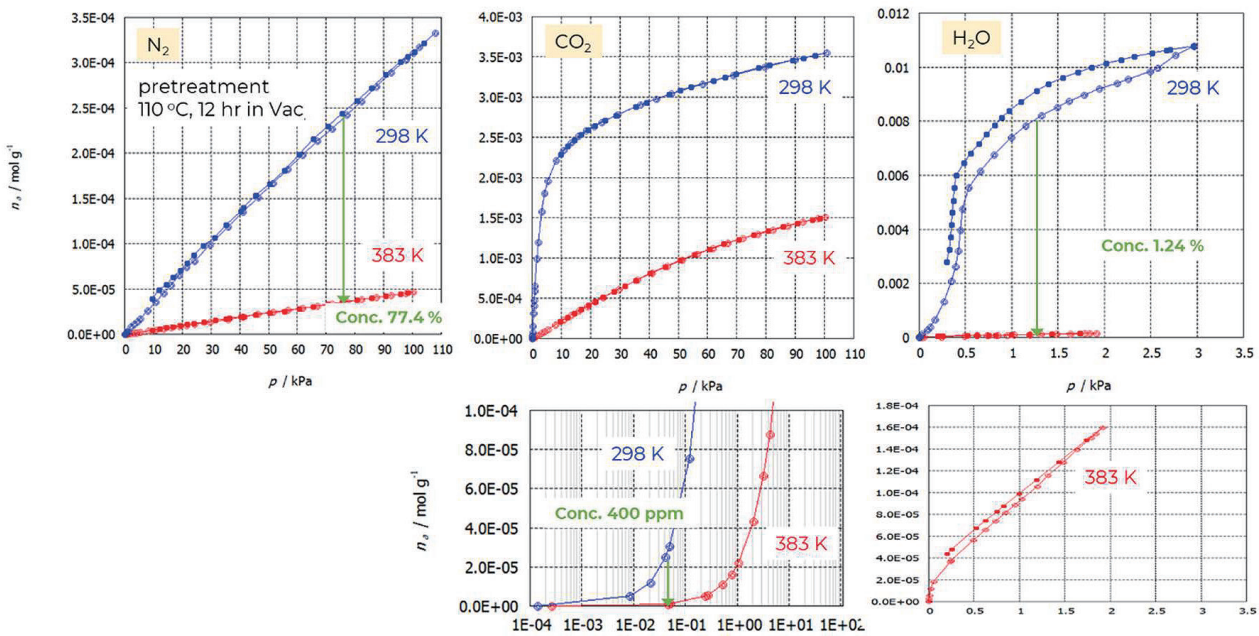

Fig.2 The adsorption isotherms of N_2, CO_2, and H_2O on CALF-20 at 25 °C and 85 °C (BELSORP MAXX)

The results of the adsorption isotherm measurements for N_2, CO_2, and H_2O on CALF-20 at 25 °C and 110 °C are shown in Fig. 2. For 400 ppm CO_2, the maximum CO_2 recovery amount when adsorbed at

25 °C and regenerated at 110 °C can be calculated as approximately 0.023 mmol g^{-1} from the differences in the respective adsorption isotherms. Similarly, the maximum recoverable amounts for 77% N_2 and 1.24% H_2O were calculated and summarized in Table 1. It was found that the maximum recoverable amounts for N_2 and H_2O on CALF-20 were 9.1 times (N_2: 0.21 mmol g^{-1}) and 371.3 times (H_2O: 8.54 mmol g^{-1}) higher than that for CO_2, respectively. These results suggest that for CO_2 separation using CALF-20, is not equilibrium separation based on differences in equilibrium adsorption amounts, but rather kinetic separation based on differences in adsorption rates. Therefore, the basic performance evaluation (screening) of the adsorbent can be considered based on the adsorption amounts at the target concentrations from the single-component adsorption isotherms. However, for actual process evaluation and verification, it is necessary to conduct multicomponent adsorption breakthrough and temperature-programmed desorption measurements under coexisting conditions of nitrogen, oxygen, and water vapor, where adsorption rates can also be considered.

Table 1 Adsorption amounts of N_2 at 77.4%, CO_2 at 400 ppm, and H_2O at 1.24% on CALF-20 at 25 °C and 110 °C, as well as the recovery amounts during the temperature change from 25 °C to 110 °C

ads. Temp.	N_2		CO_2		H_2O	
	ads. amount @77% (mmol/g^{-1})	Recovery amount (mmol/g^{-1})	Ads. amount @400 ppm (mmol/g^{-1})	Recovery amount (mmol/g^{-1})	Ads amount 124% (mmol/g^{-1})	Recovery amount (mmol/g^{-1})
25 °C	0.245	-	0.024	-	8.72	-
110 °C	0.036	0.21	0.001	0.023	0.178	8.54

The results of the CO_2 and H_2O adsorption and desorption behavior when a multicomponent gas mixture (400 ppm CO_2, 21% O_2, 1.24% H_2O (RH 40% at 25 °C), and 77.4% N_2 at 50 SCCM) was supplied to a column filled with 1g of CALF-20 at 25 °C are shown in Fig. 3. Fig. 4 provides an enlarged view of the first adsorption measurement, the first desorption measurement, and the second adsorption measurement within Fig. 3.

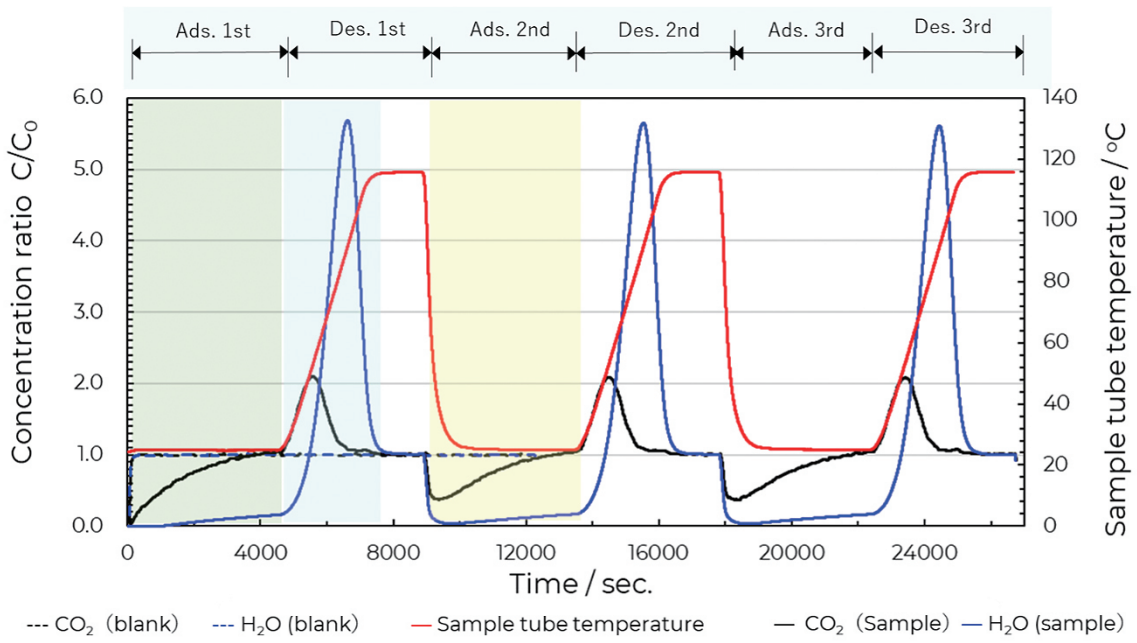

Fig.3 Adsorption & desorption behavior of CO_2 and H_2O on CALF-20 during adsorption breakthrough and temperature-programmed desorption cycles (1-3 cycles)

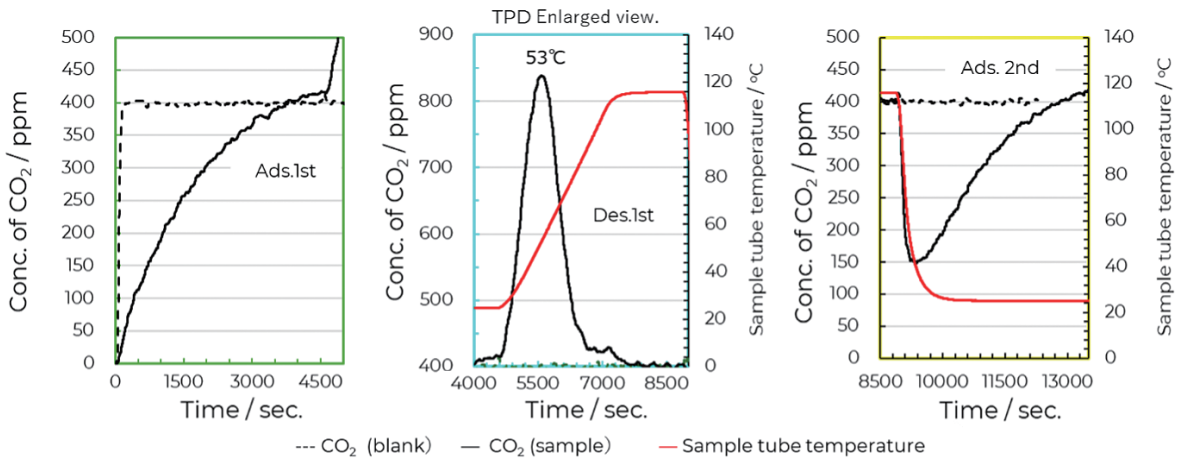

Fig.4 Enlarged view of the CO_2 adsorption behavior on CALF-20 during multicomponent adsorption breakthrough and temperature-programmed desorption cycles (1st adsorption cycle, 1st desorption cycle, and 2nd adsorption cycle)(1st adsorption cycle, 1st desorption cycle, and 2nd adsorption cycle)

From these results, it can be observed that 400 ppm CO_2, assuming atmospheric conditions, reaches the breakthrough point (128s) and the endpoint (3173s) faster than H_2O at 40% RH (at room temperature). The desorption amount at 110 °C is almost equal to the adsorption amount at room temperature, indicating a high stability of the material. The single-component CO_2 adsorption amount measured by **BELSORP MAX X** is approximately 0.023 mmol g^{-1}, while under the multicomponent gas flow, it is 0.017 mmol g^{-1}, which corresponds to about 74% of the single-component evaluation. This value remains stable even after three repeated evaluations, and the time required to reach the CO_2 breakthrough point and endpoint is almost the same. In other words, in this evaluation using CALF-20, the H_2O adsorption rate is significantly slower compared to CO_2 adsorption rate, and it does not reach the adsorption saturation. Additionally, no CO_2 desorption behavior is observed during the adsorption process, indicating that CO_2 is selectively adsorbed by the CALF-20. Furthermore, a high material stability is observed for H_2O adsorption/desorption cycles, and reproducible results are achieved over three consecutive evaluations (Table 2).

Table 2 Evaluation of CO_2 breakthrough time and end time, as well as the adsorption and desorption amounts for each cycle, and the adsorption and desorption amounts of H_2O

		1st		2nd		3rd	
		BT point	end point	BT point	end point	BT point	end point
		C/C_0=0.05	C/C_0=0.95	C/C_0=0.05	C/C_0=0.95	C/C_0=0.05	C/C_0=0.95
CO_2	time / sec	128	3137	-	3135	-	3173
	ads. amount / mmol g^{-1}	0.001	0.017	-	0.016	-	0.016
	ads. amount / mmol g^{-1}	0.017		0.016		0.016	
	des. amount / mmol g^{-1}	0.016		0.016		0.016	
H_2O	ads. amount / mmol g^{-1}	2.17		2.09		2.09	
	des. amount / mmol g^{-1}	2.13		2.12		2.10	

SUMMARY

In the evaluation of CO_2 adsorption and recovery from air under the coexistence of H_2O, assuming DAC technology 2, it was demonstrated that screening evaluation of adsorbents using single-component adsorption isotherm measurements at different temperatures with the **BELSORP MAX X** is effective. Additionally, by conducting adsorption breakthrough curve measurements and temperature-programmed desorption measurements using the **BELCAT II** in combination with CO_2 and H_2O detectors, it is possible to quantify CO_2 adsorption and desorption amounts under conditions close to practical use and understand their adsorption rate behavior. Repeating the adsorption and desorption measurement cycles also allow the evaluation of the sample's durability. In the case of CALF-20, it was shown that the CO_2 adsorption rate is faster compared to the H_2O, and repeated adsorption and desorption performance is high, indicating its potential use as an adsorbent for CO_2 in DAC technology.

Furthermore, the **BELCAT II** can be used not only for various catalyst evaluations but also for multicomponent breakthrough curve measurements using the CO_2 and H_2O detectors employed in this application note. It can also be used for single-component breakthrough curve measurements with the built-in thermal conductivity detector (TCD) and qualitative analysis with the **BELMASS II** (quadrupole mass spectrometer).

Reference

1. Jian-Bin Lin, George K. H. Shimizu et al., Science 374, 1464-1469 (2021).
2. A. Sodiq, Y. Abdullatif, B. Aissa, A. Ostovar, N. Nassar, M. El-Naas, A. Amhamed, E. T. & I., 29 (2023) 102991

EQUIPMENT

Catalyst Analyzer

BELCAT II

Measurement items

- Thermal desorption spectroscopy
- Adsorption breakthrough curve measurement

INVESTIGATION OF CO_2 ADSORPTION AND RECOVERY BETWEEN AMBIENT AND HIGH TEMPERATURE

1. INTRODUCTION

In order to achieve carbon neutrality by the year 2050, the development of Carbon dioxide Capture, Utilization and Storage (CCUS) technologies such as direct air capture (DAC) which works by directly capturing dilute CO_2 of approximately 400 ppm in the atmosphere, as well as technology which captures relatively high concentrations of CO_2 (approximately 20%) emitted from factories are underway. As one of these technologies, the separation and recovery of CO_2 can be achieved by pressure swing adsorption (PSA), in which CO_2 is adsorbed at higher pressure and desorbed at lower pressure, and temperature swing adsorption (TSA), in which CO_2 is adsorbed at room temperature (~25 °C) and desorbed at around 80-100 °C, and pressure and temperature swing adsorption (PTSA), in which both processes are taken into account (See Fig. 1).

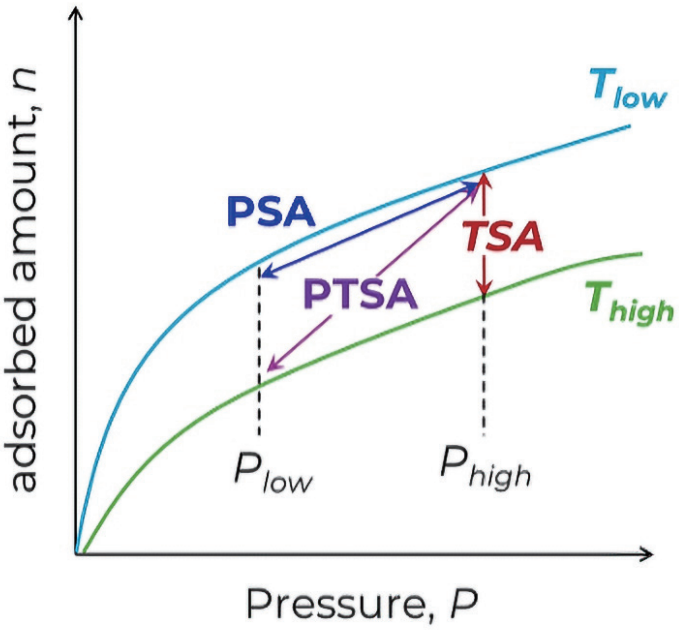

Fig.1 Process conceptual diagram for PSA,TSA,PTSA

2. EXPERIMENT

Three porous materials are investigated, which are (a) CHA zeolite (SSZ-13), a promising separation material, that was pretreated at 300 °C for 12 h, (b) MOF/PCP metal-organic structure (ZIF-8) pretreated at 150 °C for 6 h, and (c) Porous carbon (Shirasagi) pretreated at 300 °C for 8 h. The CO_2 adsorption capacity was evaluated at room temperature (25 °C) using water bath and high temperature (85 °C, 120 °C) by heater, from vacuum to 110 kPa by equipment of **BELSORP MINI X**. It is also investigated recovery amount by calculation of effective adsorbed amount, which is defined as the difference between ambient and higher temp.

3. RESULT & DISCUSSION

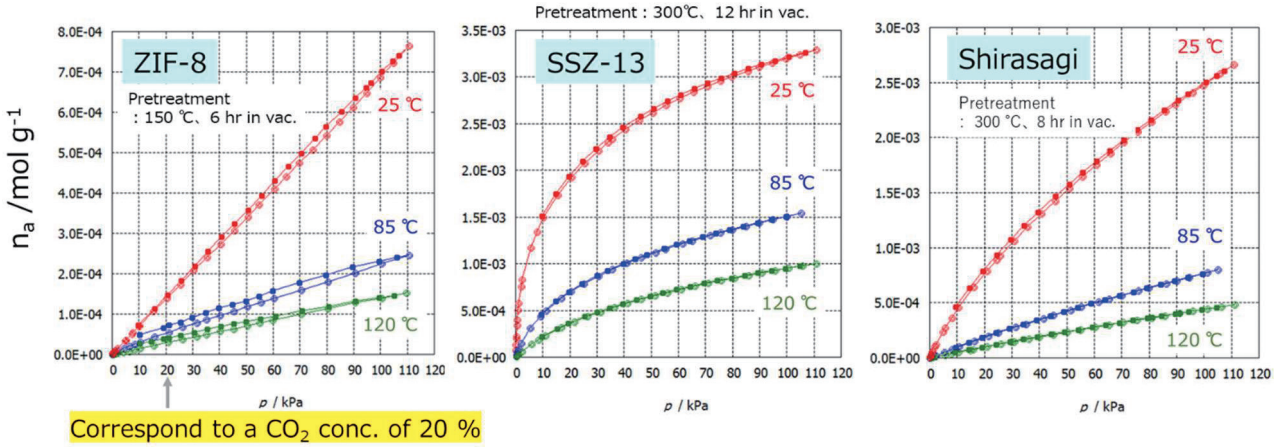

Fig.2 CO_2 adsorption isotherms @ 25 °C, 85 °C, 120 °C for each porous materials (SSZ-13, ZIF-8 and Shirasagi)

The adsorption isotherm shown in Fig. 2 expressed as CO_2 pressure (kPa) on the x-axis and CO_2 adsorbed amount (mol) per gram of the porous material on the y-axis. For example, in the case of ZIF-8, if CO_2 is adsorbed at a pressure of 20 kPa at 25 °C, and the temperature is increased to 85 °C, the adsorbent is regenerated, approximately 0.08 mmolg-1 of CO_2 will be recovered (Table 1). Comparing the three materials in a similar investigation, SSZ-13 exhibited the highest amount of adsorption and recovery at each temperature, with SSZ-13 in second and ZIF-8 the lowest amount. The single-component results in these three nanoporous materials indicate that SSZ-13 may be an effective CO_2 separation material. However, in practice, the system is required to separate CO_2 from a mixed gas, so evaluation of the adsorbed amount, recovery rate in a multi-component system in the presence of water vapor or other substances is necessary.

Table 1 Comparison of adsorption and recovery for each adsorbent

ads. Temp.	ZIF-8 (MOF/PCP)		SSZ-13 (CHA Zeolite)		Shirasagi (Activated carbon)	
	Ads amount @20kPa (mmol/g)	Recovery* (mmol/g)	Ads amount @20kPa (mmol/g)	Recovery* (mmol/g)	Ads amount @20kPa (mmol/g)	Recovery* (mmol/g)
25 °C	0.14	-	1.9	-	0.8	-
85 °C	0.06	0.08	0.7	1.2	0.2	0.6
120 °C	0.03	0.11	0.4	1.5	0.1	0.7

*Recovery is calculated assuming adsorption at 25 °C and desorption at 85 / 120 °C

Table 2 Measurement temperature range for temperature control device of each BELSORP

Model	Measuring pressure range	Measuring Temperature range	
		Water bath (O.P.)	Heater (O.P.)
BELSORP MAX X-HP	10 Pa ~ 900 kPa 1E-3 Pa ~ 110 kPa	-10 ~ 70 °C	50 ~ 550 °C
BELSORP MAX X	1E-3 Pa ~ 110 kPa		50 ~ 450 °C
BELSORP MAX G			
BELSORP MINI X	0.05 ~ 110 kPa		

4. SUMMARY

CHA zeolite (SSZ-13), MOF/PCP metal-organic structures (ZIF-8), and porous carbon (Shirasagi), which are expected as separation materials for CO_2, were pretreated at 300 °C for 12 h in vacuum and then subjected to vacuum to 110 kPa at room temperature (25 °C) and high temperature (85 and 120 °C). Evaluation of CO_2 adsorption; equipment used: **BELSORP MINI X**, 25 °C measurements; water tank used, 85 °C and 120 °C measurements; heater used and recovery evaluated.
Comparing the three materials, SSZ13 showed the largest adsorption and recovery at each temperature, with Shirasagi second and ZIF8 the smallest. The single-component results in these three nanoporous materials indicate that SSZ13 may be an effective CO_2 separation material. However, in the actual process, the system is a mixed gas system, so evaluation of the adsorption capacity in a multi-component in the presence of water vapor or other substances is necessary.

Using BELSORP series, it is possible to measure carbon dioxide adsorption isotherms of porous materials at room and elevated temperatures and easily obtain basic data (adsorption and recovery) for process studies.

EQUIPMENT

Surface area & pore size distribution analyzer

BELSORP MINI X

Measurement items

- Surface area & pore size distribution
- Gas adsorption

REPRODUCIBILITY AND EFFECTIVE ADSORPTION LOADING AMOUNT EVALUATION OF HIGH-PRESSURE CO_2 ADSORPTION ISOTHERM OF ACTIVATED CARBON (@25 °C, 120 °C)

1. INTRODUCTION

To achieve carbon neutrality by the year 2050, the development of Carbon Capture and Storage (CCS) technology, which can significantly mitigatethe CO_2 emitted into the atmosphere, is rapidly progressing. In large-scale CO_2 emission sources such as chemical plants, pre-combustion CO_2 separation and recovery technology is used, therefore it is necessary to evaluate CO_2 adsorption under conditions close to the actual environment where the temperature and pressure of the gas to be treated are high. Generally, when separating and recovering CO_2 using adsorption technology, the Pressure Swing Adsorption (PSA) process is considered. In addition, it is also important to consider CO_2 separation and recovery (and transportation) and utilization (CCU). When separating, recovering and transporting at high pressure and room temperature, and desorbing CO_2 by heating, the Pressure-Temperature Swing Adsorption (PTSA) process can be considered. Fig.1 shows the low temperature (T_{low}) and high temperature (T_{high}) CO_2 adsorption isotherms, the concept of PSA, TSA, PTSA processes, and their relationship with the effective adsorption amount. For example, effective adsorption amount of the pressure swing adsorption process (PSA②) using a material that adsorbs only CO_2 single component, the adsorption amount at adsorption pressure P_{high} and desorption pressure P_{low} on the T_{low} adsorption isotherm is defined as the difference between n4 and n3 (n4-n3). The effective adsorption amount of each process can be calculated as shown in the table in Fig.1.

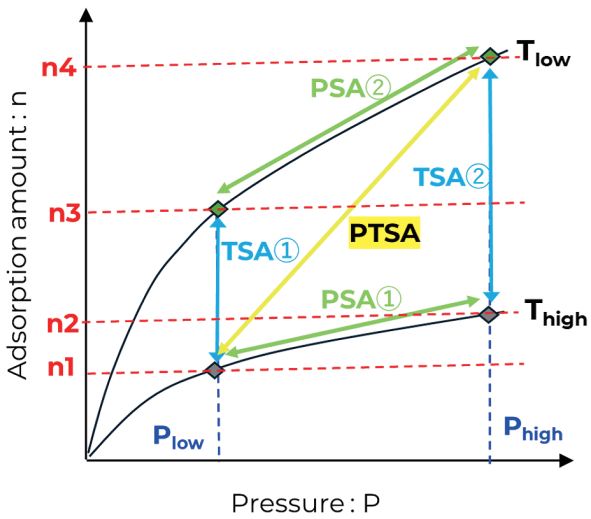

Process	Effective ads. loading amount
PSA ①	n2-n1
PSA ②	n4-n3
TSA ①	n3-n1
TSA ②	n4-n2
PTSA	n4-n1

Fig.1 PSA, TSA, PTSA process concept diagram and effective adsorption loading amount of each process.

This application note introduces examples of single-component CO_2 adsorption isotherm measurements at room temperature (25 °C) and at high temperature (120 °C) using activated carbon, which is a potential CO_2 separation material, and examples of effective adsorption amount evaluation assuming each of the adsorption processes.

1. EXPERIMENT

Activated carbon (Shirasagi LH_2c20: Osaka Gas Chemical Co., Ltd.) was pretreated by heating in vacuum at 200 °C for 3 hours, and the CO_2 adsorption (ads.) isotherm evaluation from vacuum to 900 kPa at room temperature (25 °C) and high temperature (120 °C) was performed using **BELSORP MAX X HP** (maximum measurement pressure: 900 kPa). The ads. isotherm at room temperature was measured using a water bath (measurement temperature range: -10 °C to 80 °C) and high temperature isotherms were collected using a heater (measurement temperature range: 50 °C to 400 °C). In addition, the reproducibility of CO_2 ads. and desorption (des.) measurements at high temperature (120 °C) was confirmed by repeating the measurements twice.

Furthermore, using the ads. amounts at P_{high}: 900 kPa and P_{low}: 100 kPa on the ads. isotherms at two different temperatures, the effective ads. amount for each ads. process shown in Fig. 1 was calculated.

2. RESULTS AND DISCUSSION

The ads. isotherms shown in Fig. 2 represent the equilibrium pressure of CO_2 (kPa) on the X-axis and the ads. amount of CO_2 (mmol) per 1 g of sampleon the Y-axis. The results of the effective ads. amount evaluated for each ads. process are shown in Table 1.

For example, when CO_2 is adsorbed at an ads. temperature of 25 °C and a pressure of 900kPa and then depressurized to atmospheric pressure (about 101kPa), the effective ads. amount of PSA② is 6.21 mmol/g, and the desorbed CO_2 can be recovered. When CO_2 is adsorbed at an ads. temperature of 25 °C and a pressure of 900 kPa and then heated to 120℃, the effective ads. amount of TSA② is 6.02 mmol/g. When CO_2 is adsorbed at an ads. temperature of 25 °C and a pressure of 900 kPa and then heated to 120 °C while maintaining atmospheric pressure, the effective ads. amount of TSA① is 2.09 mmol/g. In addition, when CO_2 is adsorbed at 120 °C and 900 kPa and then desorbed at atmospheric pressure, the effective ads. amount of PSA① is about 2.28 mmol/g in the first measurement and about 2.29 mmol/g in the repeated measurement, confirming good reproducibility. The PTSA process, which has the highest effective ads. amount of 8.30 mmol/g, is the most effective among all the processes. By measuring single-component ads. isotherms at room temperature and high temperature from vacuum to high pressure (900 kPa), the effective ads. amount of each ads. process can be evaluated, and in this way, it is possible to easily screen ads. materials for process consideration. However, in practice, it is necessary to evaluate breakthrough curves in multicomponent systems under coexistence with water vapor (see P4, P6 and P10).

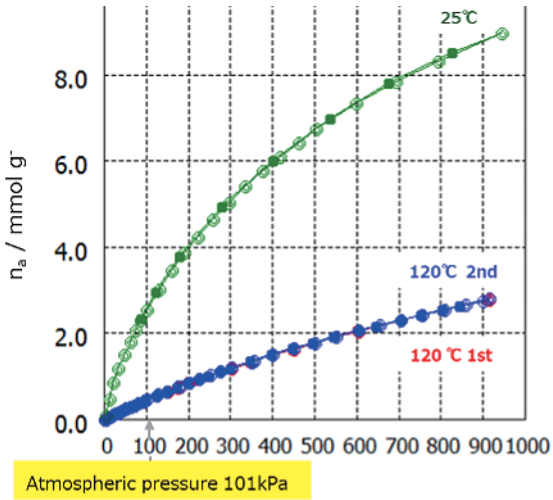

Fig.2 High-pressure CO_2 ads. isotherm measurement results of activated carbon (@25, 120 °C)

Table 1 Summary of CO_2 ads. amounts at atmospheric pressure and 900 kPa on ads. isotherms (@25 °C, 120 °C), and effective ads. amounts (recovery amounts).

	Ads. Temp. 120 °C				Ads. Temp. 25 °C	
	Adsorbed amount (mmol/g)	Effective adsorption amount (mmol/g)			Adsorbed amount (mmol/g)	Effective adsorption loading amount (mmol/g)
		900 kPa → 100 kPa	25 °C → 120 °C	25 °C, 900 kPa → 120 °C, 100 kPa		
Atmos.pressure (ca .101 kPa)	0.47	PSA ①: 2.28	TSA①: 2.09	PTSA: 8.30	2.56	PSA②: 6.21
900 kPa	1E-3 Pa ~ 110 kPa		TSA②: 6.02	—	8.77	—

References
H. Zentou, M. Aliyu, M. A. Abdalla, O. Y. Abdelaziz, B. Hoque,
A. M. Alloush, I. M. Tayeb, K. Patchigolla, M. M. Abdelnaby, Chem. Rec. vol 25, 1 (2025)

EQUIPMENT

Gas & Vapor Adsorption Analyzer (High Pressure Adsorption)

BELSORP MAX X HP

Measurement items

- Surface area
- Pore size distribution
- Gas & vapor adsorption
- (low to high pressure adsorption)

PORE STRUCTURE ANALYSIS OF CEMENT HARDENED BODY

1. OUTLINE

It is well known that the pore structure and the water content in the pores of hardened cement have a great influence on the strength and durability of concrete. In this study, we evaluated the pore volume and pore size distribution with different curing time of cement using the mercury injection method, and also evaluated the He true density and porosity using the gas displacement method.

2. MEASUREMENT RESULTS

Measuring sample: Cement (hardening time 10h ~ 4w*1)

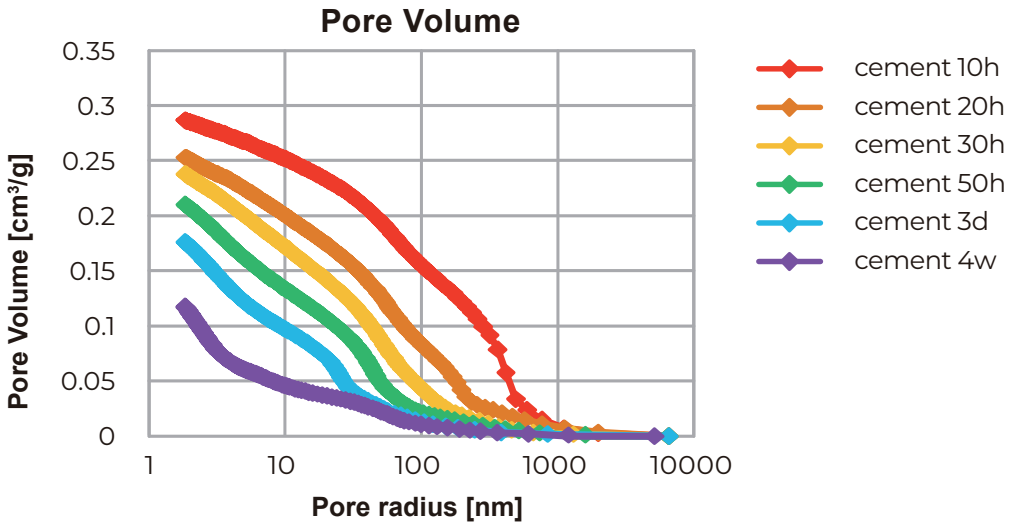

Fig.1 Cumulative pore volume by mercury injection method

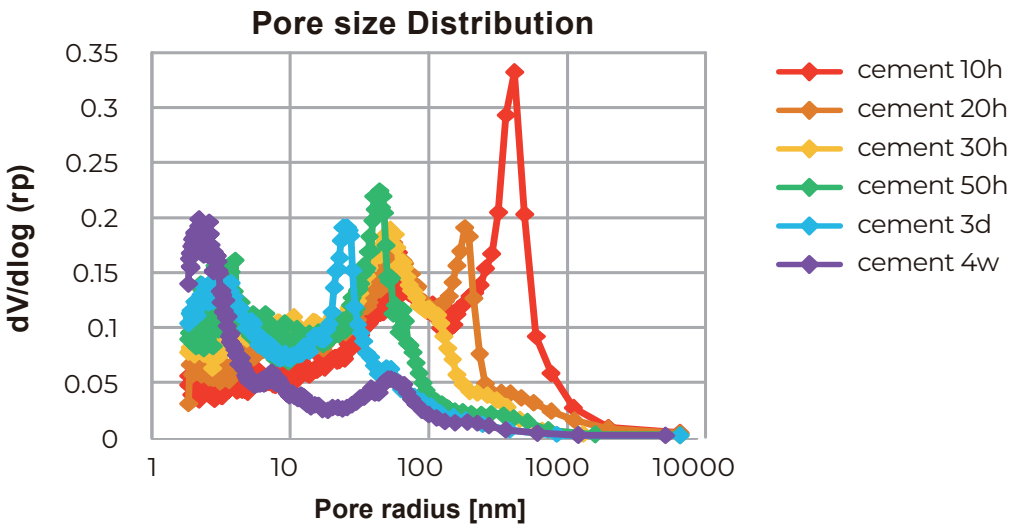

Fig.2 Pore size distribution analysis by mercury injection method

Table.1 True density and porosity of He by gas displacement method

Cement curing time	10h	20h	30h	50h	3d	4w
Density g/cm³	2.7498	2.6574	2.6136	2.5403	2.4865	2.3641
Porosity % *2	41.93	37.06	35.51	32.10	28.59	20.28

1 h:hour d:day w:week *2 Porosity with a pore diameter of 3.6 nm or more

1. RESULT & DISCUSSION

The mercury injection method showed that the pore size decreased as the curing time increased, and the pore volume also decreased.

In the early stage of cement curing, interparticle voids (macropores) are mainly formed, and then as the curing reaction progresses, the interparticle voids and pores are filled, and the pore size is considered to decrease. The He true density and porosity also tended to decrease as the curing time increased.

As described above, it is possible to obtain important data for evaluating the strength and durability of hardened cement by measuring the interparticle voids, pore size and pore volume of cement using the mercury intrusion method and gas displacement density measurement.

EQUIPMENT

Mercury porosimeter

BELPORE

Measurement items

- Pore size distribution
- Pore volume

Gas pycnometer

BELPYCNO

Measurement items

- True density
- Skelton density

MICRO-PORE EVALUATION OF MESOPOROUS Y-TYPE ZEOLITES BY CY-METHOD

1. OUTLINE

The CY method (Cheng-Yang) is an extension of the HK method and **assumes cage-type micropores in the zeolite** to calculate (Eq.1) Each terms of in the equation is defined in the following.

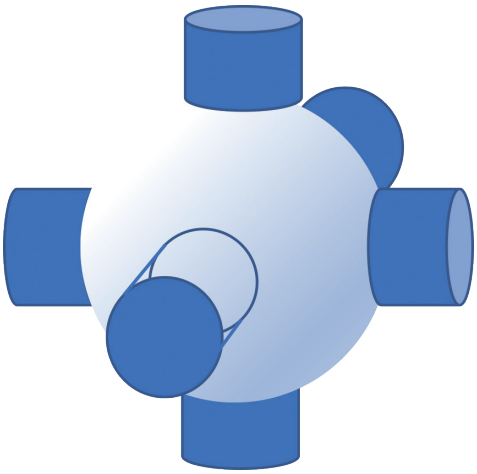

Image: Cage-type pore model

$$R\,T\,\ln\left(\frac{p}{p_0}\right) = N_{Av}\frac{6\,(N_1\,\varepsilon^*_{12} + N_2\,\varepsilon^*_{22})L^3}{(L-d_0)^3} \times\left[-\left(\frac{d_0}{L}\right)^6\left(\frac{1}{12}T_1+\frac{1}{8}T_2\right)+\left(\frac{d_0}{L}\right)^{12}\left(\frac{1}{90}T_3+\frac{1}{80}T_4\right)\right] \quad \text{(Eq.1)}$$

$$T_1 = \frac{1}{\left(1-\frac{L-d_0}{L}\right)^3} - \frac{1}{\left(1+\frac{L-d_0}{L}\right)^3}$$

$$T_2 = \frac{1}{\left(1+\frac{L-d_0}{L}\right)^2} - \frac{1}{\left(1-\frac{L-d_0}{L}\right)^2}$$

$$T_3 = \frac{1}{\left(1-\frac{L-d_0}{L}\right)^9} - \frac{1}{\left(1+\frac{L-d_0}{L}\right)^9}$$

$$T_4 = \frac{1}{\left(1+\frac{L-d_0}{L}\right)^8} - \frac{1}{\left(1-\frac{L-d_0}{L}\right)^8}$$

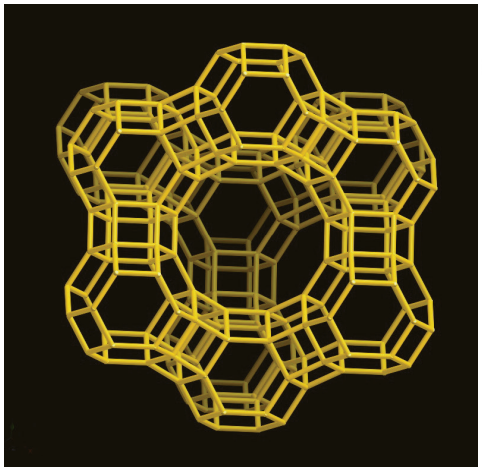

Y-type zeolite (FAU)

$$N_1 = 4\,\pi\,L^2\,N_s$$

$$N_2 = 4\,\pi\,(L-d_0)^2\,N_A$$

$$\varepsilon^*_{12} = \frac{A_s}{4\,d_0^{\,6}}$$

$$\varepsilon^*_{22} = \frac{A_A}{4\,d_A^{\,6}}$$

$$A_s = \frac{6\,m\,c^2\,\alpha_s\,\alpha_a}{\frac{\alpha_s}{\chi_s}+\frac{\alpha_a}{\chi_a}}$$

$$A_a = \frac{3}{2}\,m\,c^2\,\alpha_s\,\alpha_a$$

L : Avogadro Number

N_s , N_a: Number of atoms per unit area of adsorbent

s : adsorbent

a : adsorbate in adsorption state

ε^*_{12} : Minimum value of potential energy in adsorbent-adsorbate interaction

d_0 : Average diameter of adsorbent molecules and adsorbate atoms adsorbent

m : mass of electron

c : speed of light

$\alpha_s\alpha_a$: olarization ratio of adsorbent atoms and adsorbate molecules

x_s x_a : Magnetic susceptibility of adsorbent atoms and adsorbate molecules

It is generally known that Y-type (FAU) zeolites have increased SiO_2/Al2O3 content due to de-alumination, and that meso and macro pores are generated while maintaining the micro pore structure of the zeolite. The Y-type zeolite 320HOA(SiO_2/Al2O3=5.5) (manufactured by Tosoh Corporation) and the high-silica zeolite 390HUA(SiO_2/Al2O3=400), which is produced meso- and macropores by USY of 320HOA and de-alumization, were shown as surface SEM image (Fig. 1(1)) and crosssectional SEM image by means of BIB (Broad Ion Beam) (Fig. 1(2)) Fig. 2 shows the results of Ar@87.3K adsorption isotherms (pretreatment: 300 °C, 8 h) measured from extremely low relative pressure (p/p0=1E-8) using **BELSORP MAX.** These adsorption isotherms are classified as Type I+IV, and the hysteresis shape of 390HUA(SiO_2/Al2O3=400) confirms the development of meso- and macropores (Fig. 2).

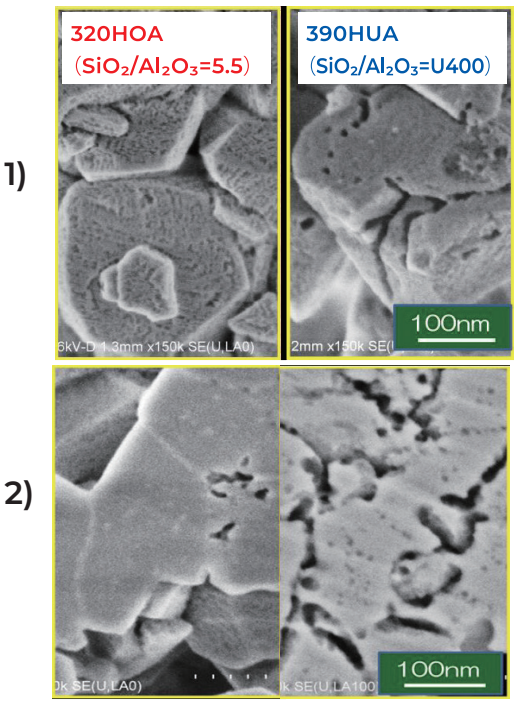

Fig.1 FAU zeolite: change in pore structure due to SiO_2/Al_2O_3
(1) HSZ particle surface image/
(2) BIB processed cross-sectional image

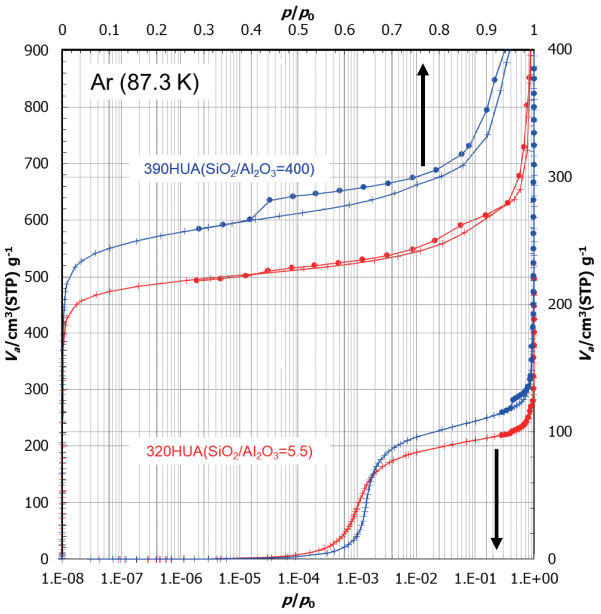

Fig.2 Adsorption isotherm of Y-type zeolite (Ar@87.4 K)

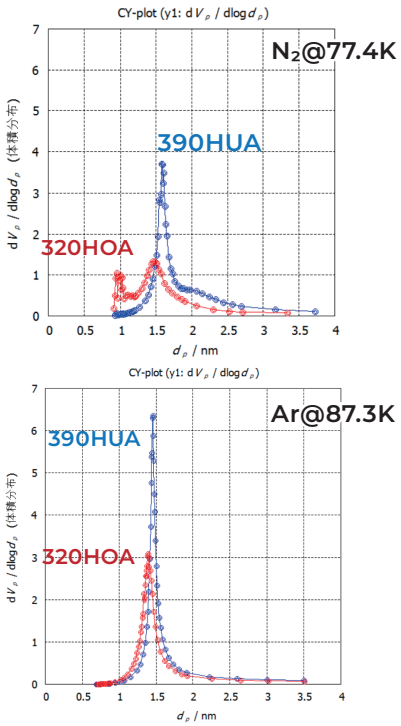

Fig.3 CY-plot

CY-plots from N_2@77.4 K and Ar@87.3 K adsorption isotherms are shown in Fig. 3. N_2 adsorbed amount gradually increases from low relative pressure and fills the micropores in Al_2O_3-rich 320HOA (SiO_2/Al2O3=5.5). From these results, there are two peaks in the CY-plot (around 1 nm: from specific strong adsorption by surface properties, around 1.5 nm: from micropore) as shown in Fig. 3 (N_2@77.4 K). On the other hand, in case of Ar@87.3K, since Ar is non-polar, the increase in adsorption behavior of both 320HOA and 390HUA is almost the same at p/p0=1E-3, regardless of the surface properties. (Fig.2) The pore size peaks of 320HOA and 390HUA at Ar@87K in Fig. 3 are 1.35 nm and 1.45 nm, respectively, indicating that the micropore size of this Y-type zeolite is slightly enlarged by USY and de-aluminum treatment.

EQUIPMENT

Gas & Vapor Adsorption Analyzer

BELSORP MAX X HP

Measurement items

- Surface area
- Pore size distribution
- Gas & vapor adsorption

INVESTIGATION OF CYLIDRICAL POROUS MATERIALS (ZEOLITE AND MESOPOROUS SILICA) BY NLDFT AND GCMC
-OPTIMUM ADSORBATE AND THEORY-

In the past, the HK (slit), SF (cylinder), and CY (cage) methods based on the adsorption potential theory were used to evaluate the pore structure of various porous materials in the micropore region due to the difference in pore structure, while the INNES (slit) and BJH (cylinder) methods based on the capillary condensation theory were used in the meso- and macropore region.
On the other hand, in recent years, computer simulation methods such as the NLDFT (Non-localized density functional theory) method and the GCMC (grand canonical Monte Carlo) method have been attracting attention for their ability to analyze pore structures from micropores to meso- and macropores using a unified theory. It is known that the pore size peaks and pore size distributions (PSD) obtained from the same adsorption isotherm are different between classical and novel analysis, and even between novel theories, because the filling pressure obtained from each theory is varied.

In the NLDFT method, the pore shape is assumed, and at the adsorption temperature and pressure, parameters such as the interaction between adsorbed molecules, the interaction between atoms constituting the adsorbent, and the interaction between adsorbed molecules and atoms constituting the adsorbent are determined, and the adsorption density in the pore is calculated using an approximate equation based on the density functional theory. The GCMC method calculates the adsorption density using a computer simulation that simulates the adsorption phenomenon by setting the same parameters as above, placing the adsorbed molecules in the virtual pore space, repeating the movement, generation, and disappearance of the adsorbed molecules, and accepting the molecules if the ground potential becomes negative (stable), and restoring the molecules if the ground potential is the opposite.
Fig.1 is a relationship between adsorption densities and relative pressure for local isotherm of 4 nm (left) and 10nm (right) by NLDFT and GCMC calculation. From these results, it can be seen that the NLDFT method underestimates the adsorbed phase density and overestimates the filling pressure compared to the GCMC method (Fig. 1). In other words, the NLDFT method can be considered overestimates the pore volume and underestimates the pore size.

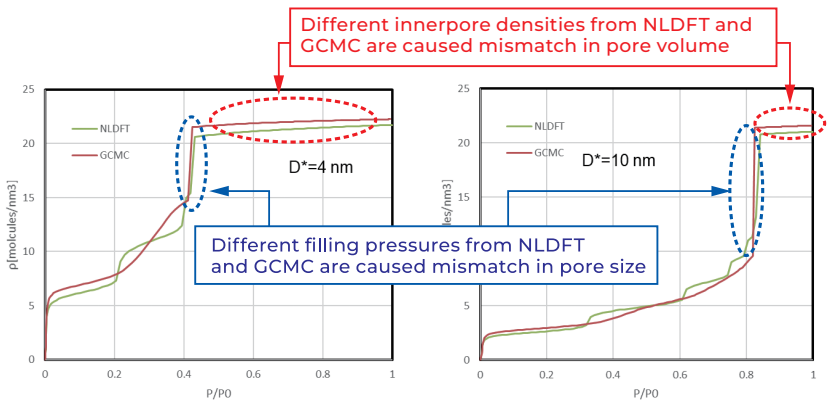

Fig.1 Local isotherms of 4 nm and 10 nm by NLDFT and GCMC (adsorbed branch Ar@87. 3K)

Here, we will discuss which theory is more suitable for PSD analysis, the NLDFT method or the GCMC method. Also, although Ar adsorption is the adsorbent proposed in IUPAC 2015, to what extent is N_2 adsorption useful? We will analyze N_2 (77.4K) and Ar (87.3 K) real adsorption isotherms of mesoporous silica MCM41, MFI (10-membered ring), and MTW (12-membered ring) zeolites with cylinder pores, and examine them concretely.

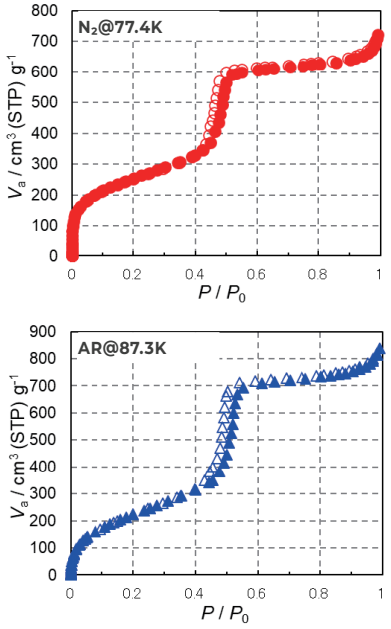

Fig.2 Adsorption isotherms of MCM41 (N_2@77.4 K, Ar@87.3 K)

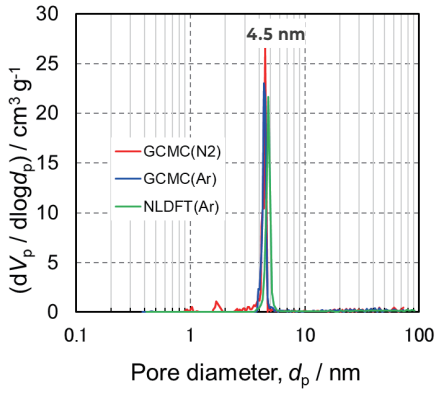

Fig.3 PSD of MCM41 (N_2@77.4 K, Ar@87.3 K)

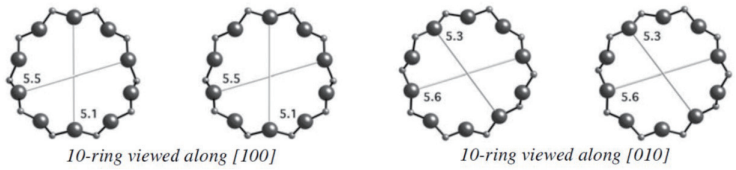

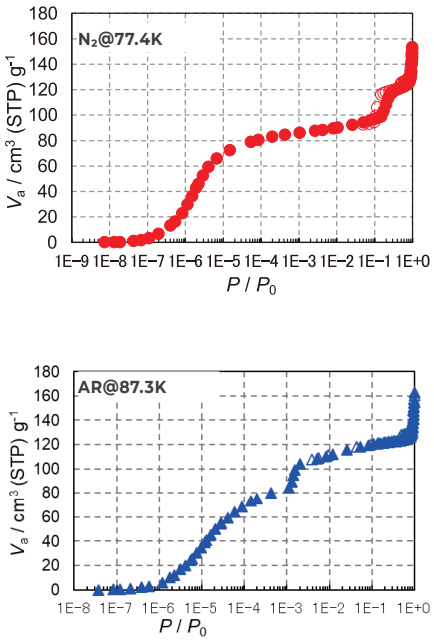

Fig.4 Adsorption isotherms for MFI 1000H (N_2@77.4 K, Ar@87.3 K)

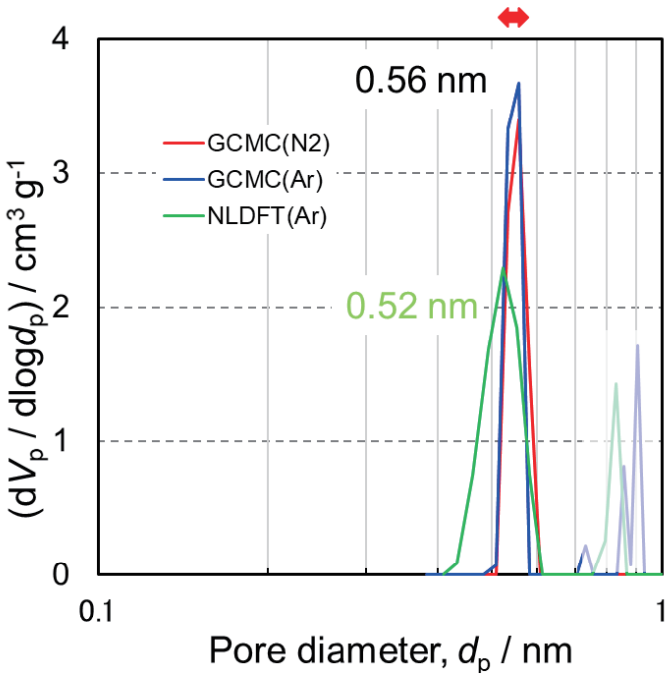

Fig.5 MFI pore structures provided by IZA and Pore size distribution from GCMC and NLDFT of MFI 1000H (N_2@77.4 K,3 Ar@87.3 K)

The mesoporous silica MCM41 N_2@77.4 K and Ar@87.3 K adsorption/desorption isotherms (Fig.2) are classified as Type IVb, indicating the presence of mesopores. Fig.3 shows the PSD of MCM 41 calculated by GCMC and NLDFT method from Ar@87.3 K isotherm as well as PSD by GCMC from N_2@77.4 K isotherm. This confirms that all results of the analysis of PSD by the GCMC and NLDFT methods using N_2@77.4 K and Ar@87.3 K adsorption isotherms for mesoporous MCM41 are in good agreement.

The microporous MFI (10-membered ring) zeolite 1000H (Si/Al=500) with N_2@77.4 K, Ar@87.3 K adsorption/desorption isotherms (Fig.4) are classified as Type I, indicating the presence of micropores. Fig.5 shows PSD for each adsorbate N_2@77.4 K and Ar@87.3 K calculated by the GCMC method and the NLDFT method. The pore size distribution analysis by the GCMC method is in good agreement with the pore size obtained from the XRD provided by IZA (International Zeolite Association) shown in Fig 5. On the other hand, the pore size distribution from the NLDFT method is broad due to its kernel problem, showing a pore size distribution of 0.4-0.5 nm, which does not exist in reality.

In Fig. 6, N_2@77.4 K and Ar@87.3 K adsorption/desorption isotherms for MFI (25H) of Si/Al=12.5 were compared with those for MFI (1000H) of Si/Al=500. The isotherms for 25H show a gradual increase in adsorption branch from low relative pressure and micropore filling due to the involvement of the N_2 quadrupole and strong adsorption on the zeolite pore surface, whereas for 1000H, the adsorption increases rapidly at around p/p0=1E-6 and it can be seen the micropore filling is taking place. For the Ar@87.4 K isotherm, since Ar is non-polar, the behavior of the amount of adsorbate increases around p/p0=1E-6 for both 25H and 1000H, regardless of the surface condition. 25H N_2@77.4 K by the GCMC method (Figure7), N_2 molecules are strongly adsorbed on Al+ sites due to their quadrupole moment, resulting in a small pseudo-pore distribution around 0.4 nm. The pore size distribution of 25H from the NLDFT method by Ar molecule is broad 0.4-0.5 nm not existing in reality just same as 1000H.

From the above, it can be said that for MFI zeolites with 10-membered rings, the GCMC method using N_2 adsorption gas can analyze the appropriate pore distribution (>0.5 nm) except for the Al+ site, while the GCMC method using Ar adsorption gas can analyze the appropriate pore distribution and pore volume.

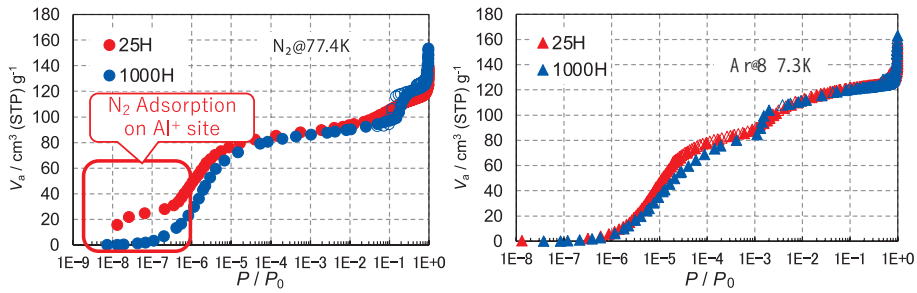

Fig.6 Adsorption isotherms of MFI 25H and 1000H (N_2@77.4 K, Ar@87.3 K)

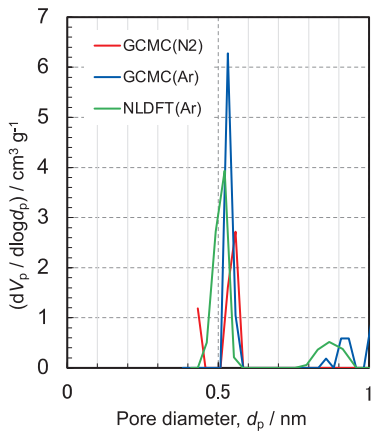

Fig.7 Pore distribution (pore volume) of MFI25H (N_2@77.4 K, Ar@87.3 K)

From the GCMC and NLDFT pore distribution analysis of MTW (ZSM-12, 12-membered ring) Ar@87.3 K (Figure8), the GCMC pore size distribution agrees well with the pore structure shown by IZA, while the NLDFT pore size distribution is underestimated due to its kernel problem (Figure 1). The pore volume of the NLDFT method was overestimated to 0.17 cm^3 comparing to an ideal pore volume "0.14 cm^3" of the 0.58 nm cylinder shape assuming a molecular diameter of 0.34 nm of Ar molecule. The pore volume calculated from GCMC is as same as the ideal volume.

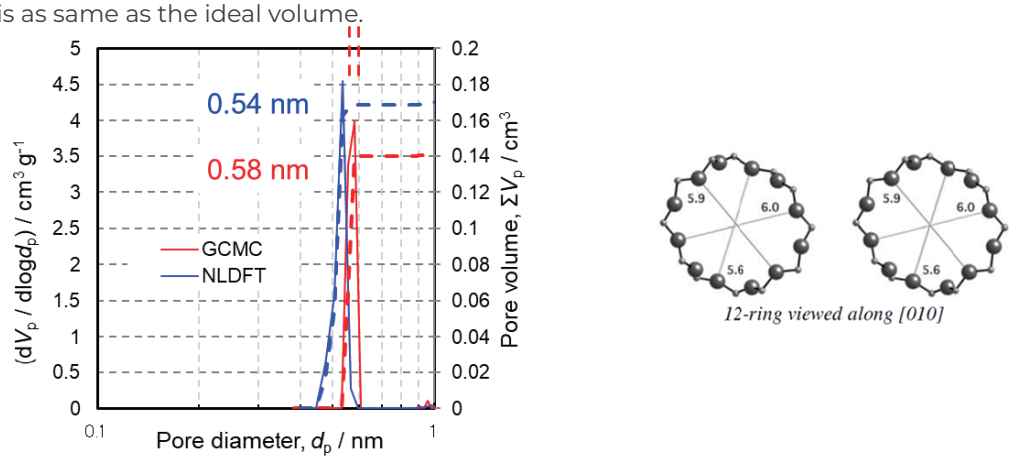

Fig.8 Pore distribution and cumulative pore volume distribution of MTW 12-membered rings by GCMC and NLDFT methods [ΣVp] 3(Ar@87.3 K)

In summary (Table 1), the NLDFT and GCMC methods can be used to evaluate the pore size distribution of materials with cylinder-shaped mesopores, regardless of whether the adsorbate is N_2 or Ar. For zeolites with micro-pores of the same shape, the Ar adsorption GCMC method is the best method to analyze the pore distribution when the pore size is larger than 0.4 nm (confirmed separately by an 8-membered ring zeolite; not shown in this report), and the N_2 adsorption GCMC method can also analyze the pore size distribution (>0.5 nm) except for zeolite with the Al cation site rich surface. In addition, the NLDFT method underestimates the pore distribution and overestimates the pore volume, regardless of the adsorbent, when evaluating the pore structure of microporous zeolites, so the GCMC method is recommended.

Table 1 Evaluation of pore structure by NLDFT/GCMC method and N_2 and Ar for porous materials with cylinder shape.

	NLDFT Method		GCMC method	
	N_2	Ar	N_2	Ar
Pore size > 2nm (mesopore)	○	○	○	○
Pore size > 0.5nm (10-membered ring micropore)	△	△	○	○
Pore volume	×	×	○	○
Al^+ site rich surface	△	△	△	○

EQUIPMENT

Gas & Vapor Adsorption Analyzer (High Pressure Adsorption)

BELSORP MAX X SERIES

Measurement items

- Surface area
- Pore size distribution
- Gas & vapor adsorption

INCREASED ACCURACY IN THE PORE STRUCTURE ANALYSIS OF ACTIVATED CARBONS USING A NEW GCMC KERNEL BASED ON A SLIT-PORE MODEL WITH CARBON SURFACE HETEROGENEITY

SUITABLE APPLICATIONS

Catalyst | Adsorbents | Battery cell | Electronic component

APPLICABLE MATERIAL

Carbon

New carbon slit GCMC kernel with roughness surface

MEASUREMENT & ANALYSIS

The N_2@77.4K and Ar@87.3K adsorption isotherms of activated carbon fiber (ACF) from Kuraray Chemical (FT300-25) were measured using BELSORP MAX series (MICROTRAC). The pore size distribution of the carbon fiber was analyzed and compared using a carbon slit GCMC kernel with a roughness surface, a smooth surface, and a QSDFT based carbon slit kernel.

RESULT

The simulated adsorption isotherm obtained from the roughness kernel showed good agreement and a better fit with the experimental adsorption isotherm.

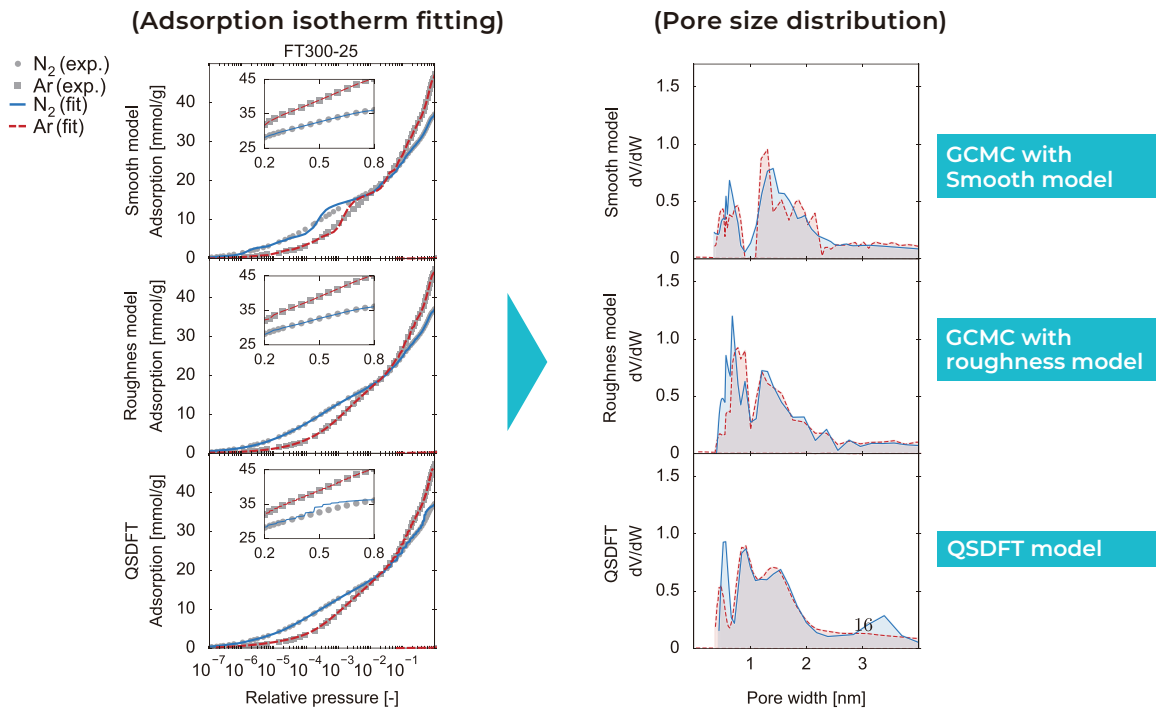

GCMC WITH SMOOTH MODEL

A simulated adsorption isotherm based on the use of smooth kernel exhibits partially different behavior from the experimental data, resulting in a valley in the pore size distribution at pore diameters of approximately 0.9 nm.

GCMC WITH ROUGHNESS MODEL NEW

The simulated adsorption isotherm using updated kernel with surface roughness provides a better match with the experimental isotherm and represents a more accurate pore size distribution.

QSDFT NEW

The PSDs derived from the QSDFT method also showed systematic valleys and peaks, indicating insufficient results.

Reference; S. Hiraide et. al. Adsorption, 29, PP387-399 (2023)

EQUIPMENT

High-Precision gas / vapor adsorption measurement system

BELSORP MAX X SERIES

Measurement items

- Surface area
- Pore size distribution
- Gas & vapor adsorption

High-precision gas adsorption measurement system

BELSORP MAX G

Measurement items

- BET surface area
- Pore size distribution
- Gas adsorption

The new GCMC kernel with roughness surface and **QSDFT kernel** are implemented in the analysis software BELMaster and is suitable for use with the data from **BELSORP MAX G** and **BELSORP MAX X series**.

POROUS METAL COORDINATION POLYMER (MOF/PCP) MATERIALS

-SPECIFIC SURFACE AREA AND PORE STRUCTURE ANALYSIS-

01. PREFACE

Recently, porous metal-organic frameworks (MOFs)/porous coordination polymer (PCP) materials have been widely studied. As shown in the figure below, the pore structure of this material can be freely designed by selecting metal ions and ligands. PCPs are expected to be used for gas storage, gas separation, and selective catalytic reactions because of their regular pores and large pore size due to their crystalline structure. In addition to MOF/PCP materials with fixed pores, a number of materials with flexible pores have been synthesized, and the change in pore structure due to adsorption has been interestingly reported by combining adsorption and X-ray structural analysis data.

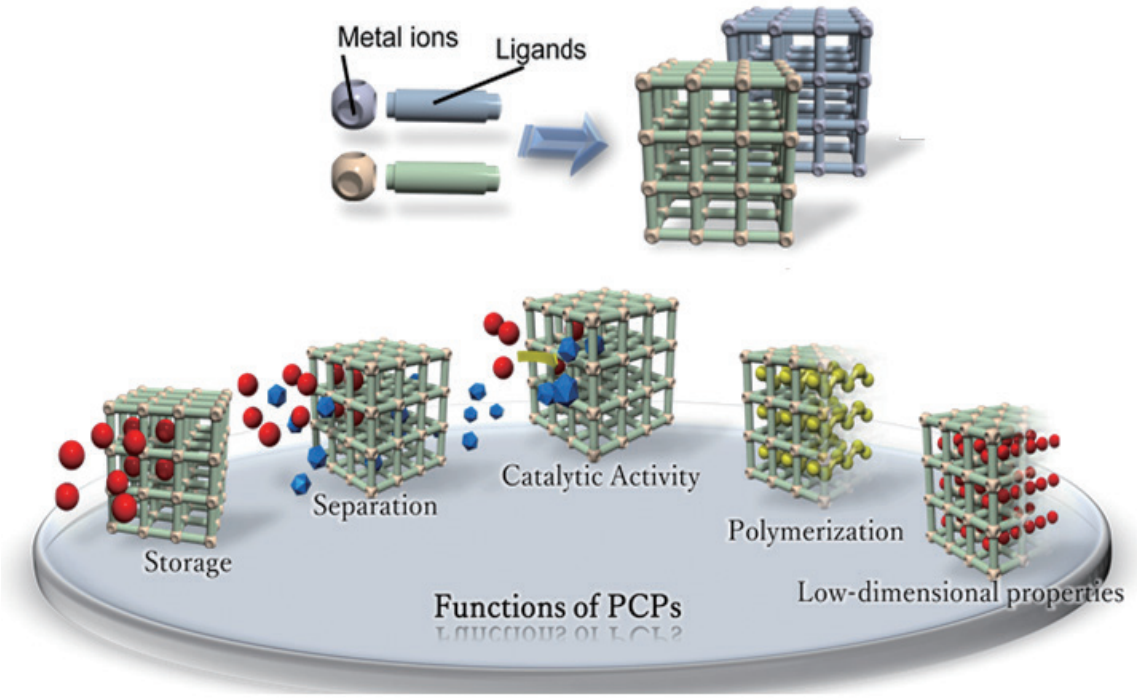

Ref: Prof. Susumu Kitagawa and Ryotaro Matsuda

However, structural analysis of such novel porous materials based on existing gas adsorption theory requires caution. Firstly, the exposed surface atoms of the solid adsorbent are not homogeneous, consisting of metal and ligands, and secondly the pore walls are single molecule walls, which limit the interaction with adsorbed molecules but cause interaction with molecules adsorbed in neighbouring pores. When such specific adsorption occurs, applying existing theories of adsorption analysis becomes problematic.

02. SPECIFIC SURFACE AREA ANALYSIS

The Brunauer-Emmett-Teller (BET) method is the most common method for the evaluation of specific surface areas. It is applicable to sorption isotherms Type II and Type IV and the evaluation is carried out in the relative pressure range *P/Po* from 0.05 to 0.30 as recommended by IUPAC. BET specific surface area is a physical quantity calculated from nitrogen, krypton or argon gas adsorption isotherms, and therefore, it does not correspond to the geometric surface area, or the surface area calculated from X-ray structure analysis. However, the BET specific surface area is one of the most important parameters in evaluating the adsorption capacity of a material.

The gas adsorption isotherms of MOF/PCP materials show mainly type I isotherms (Fig. 1). Applying standard BET relative pressure range will result in bad correlation coefficient and negative C value, hence wrong BET surface area values.

To solve this issue, Rouquerol et al. recommend obtaining the maximum relative pressure for type I isotherms from the Volcano plot (Fig. 2) and selecting a region with good linearity and a positive C value (Fig. 3).[1,2]

In the case of MOF/PCP materials, N_2 as well as Ar adsorption analysis can be used, while Ar is recommended for analysing specific BET surface area and pore size distribution. It should be noted that the adsorptive (N_2, Kr or Ar) must be reported and these BET surface area values should only be compared using the same adsorptive.

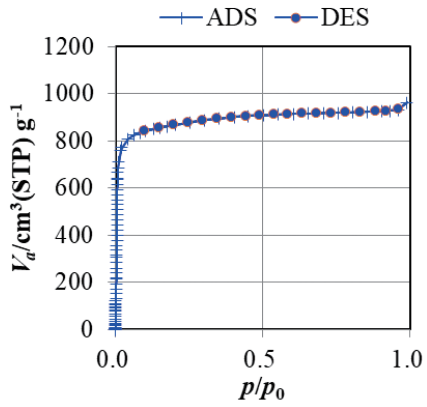

Fig.1 N_2 adsorption Isotherm of MOF-5 at 77 K

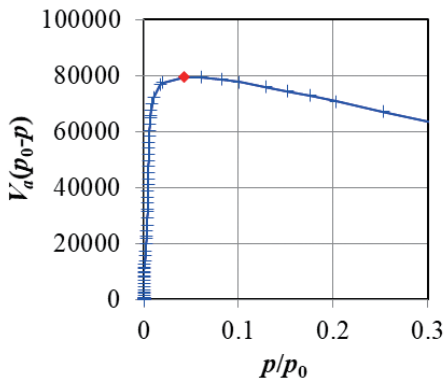

Fig.2 Volcano plot of Fig.1 isothermK

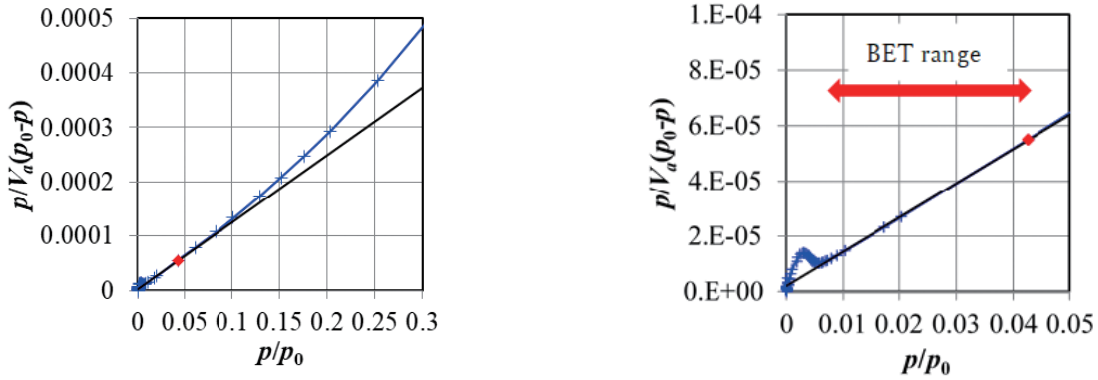

Fig.3 BET plot(◆BET range limit)

Table 1 Results of MOF-5 from BET plot

BET analysis range	0.00712-0.0426	*p/po*
as,BET	3508.2	[$m^2 g^{-1}$]
C	607.94	

1) J. Rouquerol, P. Llewellyn and F. Rouquerol, *Stud. Surf.* Sci. Catal., 2007, 160, 49–56.
2) ISO9277:2010, JIS Z8830:2013

03. PORE SIZE DISTRIBUTION ANALYSIS

The gas adsorption isotherms can be analysed by various analytical theories considering different pore models and adsorbent surface. Activated carbon and zeolite with micropores can be analysed as slit/cylinder/cage type pore structures whose solid surface is composed of carbon and oxygen atoms (metal oxides). The porous metal-coordination polymer MOF/PCP materials can be designed as a variety of pores due to their defined crystal structure. Its solid surface mainly consists of metal/carbon/hydrogen/nitrogen/oxygen atoms, etc., and the surface energy cannot be simplified. The pore shape is triangular/square/rhombic/cage-shaped, and the pore structure is one-dimensional to three-dimensional. In addition, not only materials with fixed pore structures, but also materials whose pore structures can be flexibly changed by adsorption have been developed. Therefore, it is difficult to determine the pore distribution of MOF/PCP materials from gas adsorption, and it is common to analyse the pore structure from X-ray structure analysis.

However, the adsorption isotherm contains the pore information of the adsorbent. If the pore geometries of materials are similar but different pore sizes (e.g. due to different ligands), the relative comparison is possible by the general pore distribution theory. To evaluate the molecular sieving effect by controlling the pore size of MOF/PCP materials, it is possible to determine the accurate molecular sieve pore size by plotting the molecular size of probe (adsorptive) and the adsorbed amount (pore volume).

For MOF/PCP materials whose pore structure is not changed by adsorption, relative comparison can be made using pore distribution analysis by GCMC method. In this case, it is preferable to use Ar as an adsorptive. Since the surface energy of MOF/PCP materials is not uniform - due to the determination of various metal atoms and various ligands - and Ar adsorption (87 K) has a weak adsorbent-adsorbate interaction, it provides pore information that reduces the influence of the surface energy. For the pore structure, the pore shape is determined from the X-ray structural analysis and the model with the closest pore structure is selected from the slit/cylinder/cage type pore model.

The t-plot from the nitrogen adsorption isotherm can be used to calculate the pore volume and external surface area (primary particle size).

04. EXAMPLES OF ADSORPTION ISOTHERM ANALYSIS OF VARIOUS MOF/PCP

The adsorption isotherms are measured by **BELSORP MAX series** (MICROTRAC) and surface area and pore size distribution are examined by the analysis software BELMASTER (ver.7.3.2.0).

04.1 MOF-5

Basolite Z100	$Zn_4O(BDC)_3$
Pore wall atoms	Pore wall atoms : oxygen, carbon, hydrogen
Pore structure	Cage type
X-ray structural analysis Unit cell	25.832 Å (a,b,c)
Assumed pore diameter	1.29 nm
Density(ρ_{UC})	1022.7×10^{-23} g / UC
Density(ρcage)	5 cage / UC

https://www.chemtube3d.com/mof-mof5/
https://www.chem-station.com/chemglossary/2021/01/mof-5-mof.html

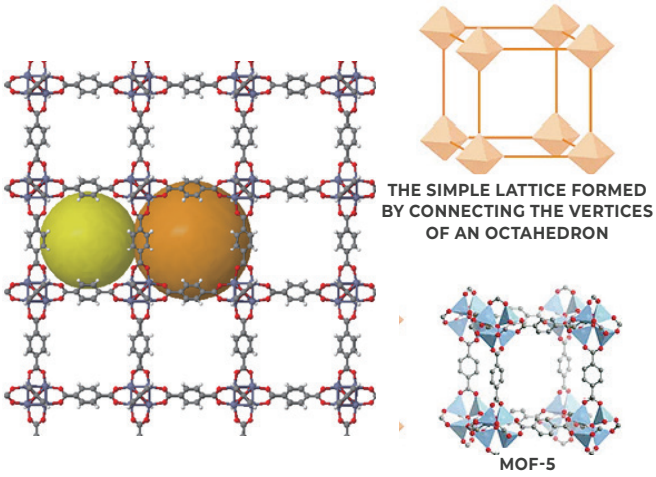

Fig.4 Structure of MOF-5

This material has micropores after the guest molecules are removed by vacuum heat pretreatment at 300 °C. The pore structure belongs to the cage type, and the pore walls are mainly formed by eight locations, which are the vertices of a cube, and the ligands connecting them. Its pore capacity is much larger than that of conventional activated carbon and zeolite.

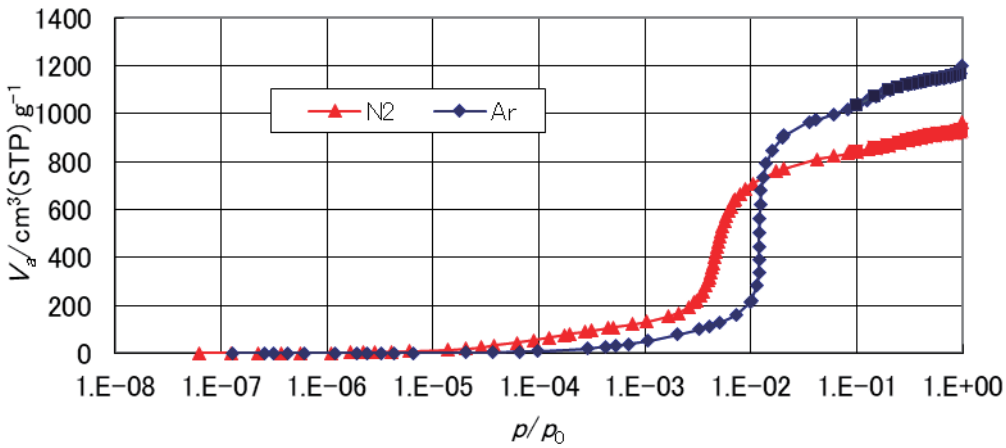

Fig.5 Adsorption isotherms of N_2 at 77 K and Ar at 87 K on MOF-5

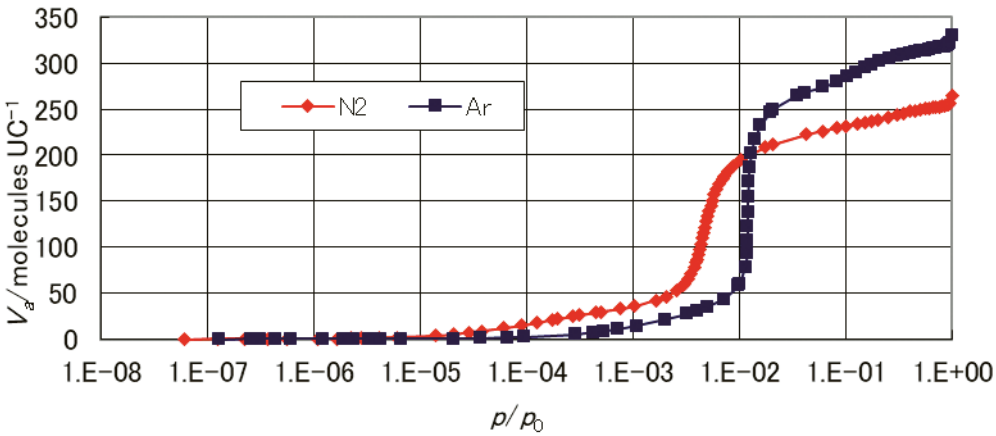

Fig.6 Adsorption isotherms of N_2 at 77K and Ar at 87K on MOF-5
[Y-axis : Uptake in molecule number / UC]

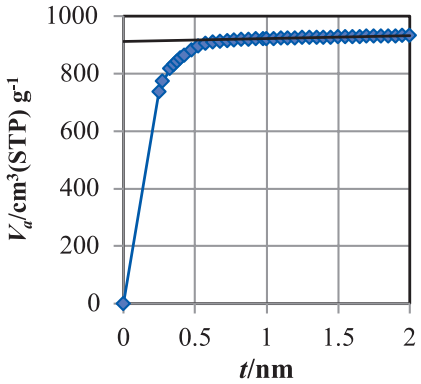

Intercept:	911.8 cm³(STP)/g
Vmicro:	1.41 cm³/g
as,BET	15.6 m²/g

Fig.7 t-plot from N_2 isotherm

Table 2 Calculation physical parameters from gas adsorption isotherms

Adsorption quality			N_2	Ar
Specific surface area [1]	**[m² g⁻¹]**	as,BET	3508	3677
C value [1]			607.9	605.5
Total pore volume [2]	**[cm³ g⁻¹]**	V_{pore}	1.49	1.53
Pore volume [3]	**[cm³ g⁻¹]**	V_{micro}	1.41	-
Adsorption capacity [4]	**[molecule UC⁻¹]**	V_{UC}	250.5	-
Adsorption capacity [5]	**[molecule cage⁻¹]**	V_{cage}	50.1	-
External surface area [3]	**[m² g⁻¹]**	$a_{s,EXT}$	15.6	-
Average particle size [6]	**[μm]**	d_P	5.2	-

1) BET plot
2) Gurvich rule (p/p_0 = 0.99) ρl : liquid density of adsorbate
3) t-plot
$V_{micro} \fallingdotseq V_{pore}$: Total pore volume is assumed to be micropore volume.
4) $V_{UC} = V_{micro} \times \rho l / MWa \times \rho UC \times NA = Vg,_{micro} / 22414 \times \rho_{UC} \times N_A$
5) $V_{cage} = V_{UC} / \rho_{cage}$
6) $d_P = 6 / [as_{EXT} \times \rho_{UC} / (a_{UC}^3 \times 10^{-24})]$

The average particle size is calculated from the external specific surface area and density calculated from the t-plot assuming that the crystallites are cubic.

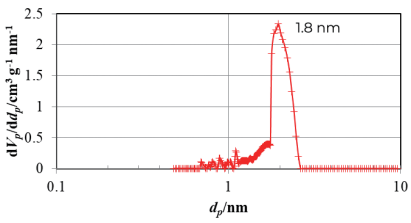

Fig.8 Pore size distribution from GCMC method (Ar, Cage)
[Kernel: Metal Oxide for microporous solid]

The pore distribution was calculated to be 40% larger than the pore diameter (1.29 nm) estimated from the crystal structure. This is thought to be due to the lower density of the wall in the MOF-5 structure compared to the cage-type model. When the interaction between adsorbed molecules and the wall is low, the pore diameter is calculated to be larger.

4.2 HKUST-1

Basolite C300	$Cu_3(btc)_2$
Pore wall atoms	Pore wall atoms: oxygen, carbon
Pore structure	Cage type (2 types)
X-ray structural analysis Unit cell	26.303 Å
Assumed pore diameter	0.52, 1.14 nm
Pore wall ratio	50, 36.6
Density(ρ_{UC})	1623×10^{-23} g / UC
Density(ρ_{cage})	8 × 5 cage / UC

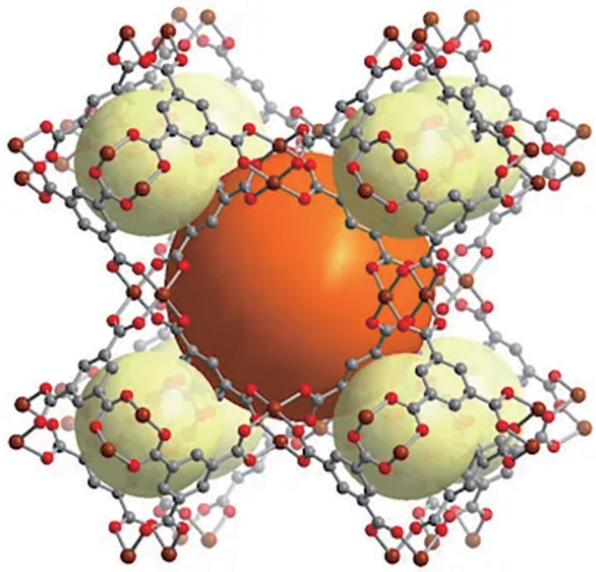

Fig.9 HKSUT-1 unit cell tructure

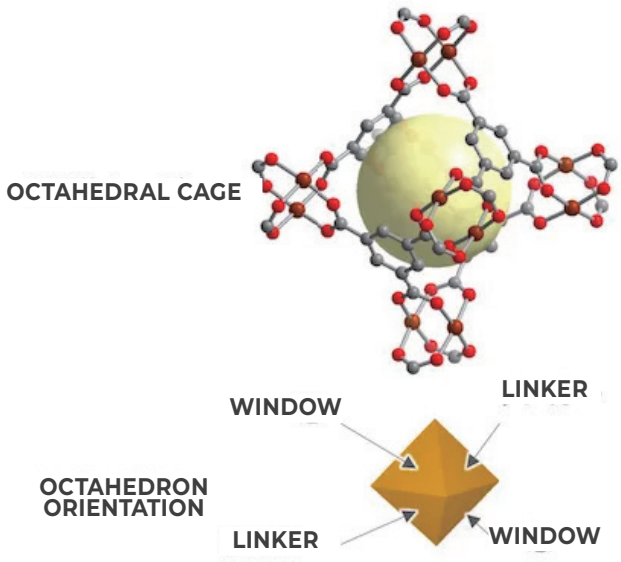

Fig.10 HKUST-1 Small cage structure

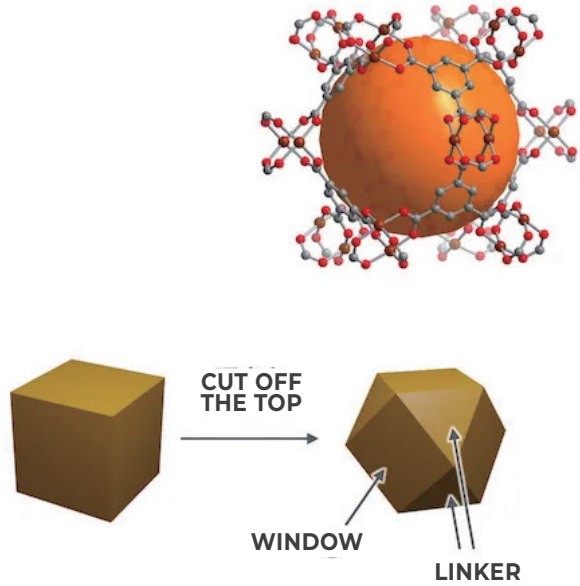

Fig.11 HKUST-1 Large cage structureture

https://www.chemtube3d.com/mof-hkust-1-2/
https://www.chem-station.com/chemglossary/2021/01/hkust-1.html

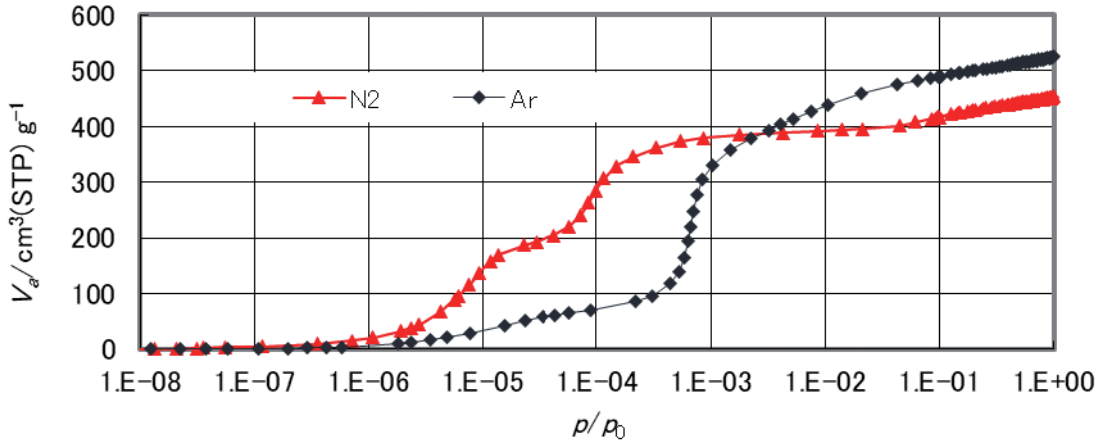

Fig.12 Adsorption isotherms of N_2 at 77 K and Ar at 87 K on HKUST-1

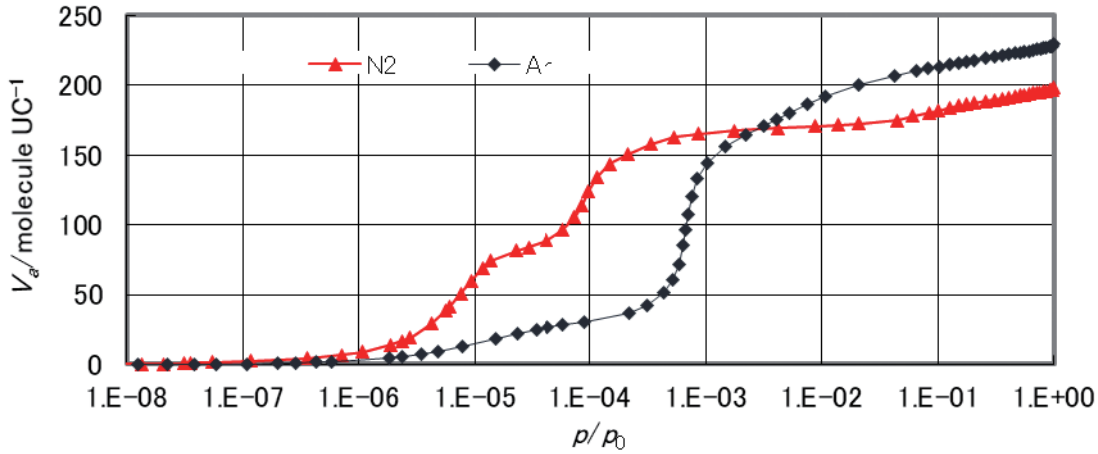

Fig.13 Adsorption isotherms of N_2 at 77 K and Ar at 87 K on HKUST-1
[Y-axis : Uptake in molecule number / UC]

Table 3 Calculation physical parameters from gas adsorption isotherms

Adsorption quality			N_2	Ar
Specific surface area [1]	**[m² g⁻¹]**	$a_{s,BET}$	1695	1759
C **value** [1]			39587	1622
Total pore volume [2]	**[cm³ g⁻¹]**	V_{pore}	0.702	0.669
Pore volume [3]	**[cm³ g⁻¹]**	V_{micro}	0.689	-
Adsorption capacity [4]	**[molecule UC⁻¹]**	V_{UC}	194	-
External surface area	**[m² g⁻¹]**	$a_{s,EXT}$	5.01	-
Average particle size [6]	**[μm]**	d_P	24.4	-

1) BET plot
2) Gurvich rule (ρ/ρ_0 = 0.99) ρl : liquid density of adsorbate
3) t-plot
$V_{MICRO} \fallingdotseq V_{PORE}$: Total pore volume is assumed to be micropore volume.
4) $V_{UC} = V_{MICRO} \times \rho l / MWa \times \rho UC \times N_A = V_{g,\ micro} / 22414 \times \rho UC \times N_A$
5) $d_p = 6 / [asEXT \times \rho UC / (a_{UC}^3 \times 10^{-24})]$.

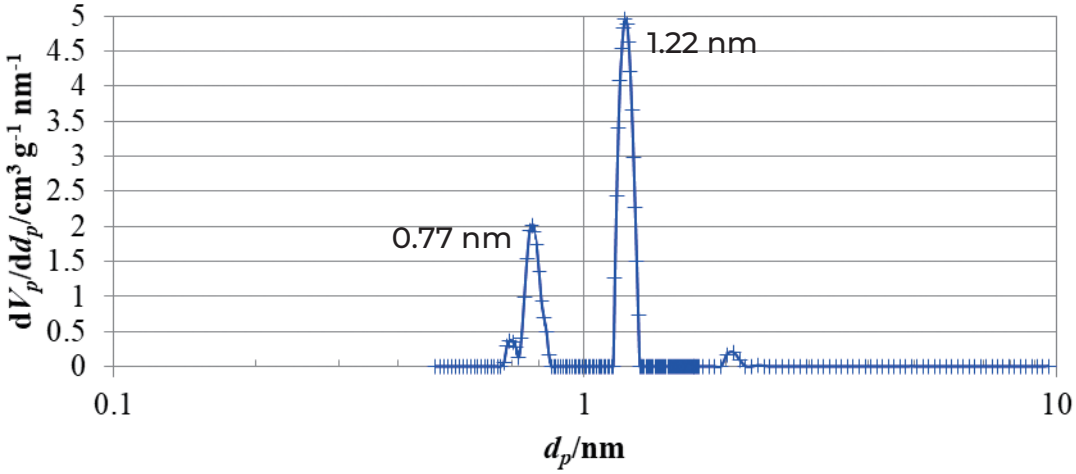

Fig.14 Pore size distribution from GCMC method (Ar, Cage)
[Kernel : Metal Oxide for microporous solid]

The pore size distribution was bimodal as inferred from the crystal structure. The pore diameters were calculated to be 48% and 7% larger than those estimated from the crystal structure of 0.52 and 1.14 nm, respectively. This is probably due to the lower density of the wall in HKUST-1 compared to the cage-type model. When the interaction between adsorbed molecules and the wall is low, the pore size is calculated to be larger.

EQUIPMENT

Gas & Vapor Adsorption Analyzer

BELSORP MAX X SERIES

Measurement items

- Surface area
- Pore size distribution
- Gas & vapor adsorption

REPEATED PERFORMANCE EVALUATION OF WATER VAPOR ADSORPTION AND DESORPTION FOR PCP/MOF (POROUS METAL ORGANIC FRAMEWORK)

01. INTRODUCTION

The adsorption of water by porous solids is important for many applications requiring capture and release of water. Some key applications include dehumidification, thermal batteries, and the delivery of drinking water to remote areas (1). Generally, there are three key considerations when designing adsorbent materials suitable for water storage, including:

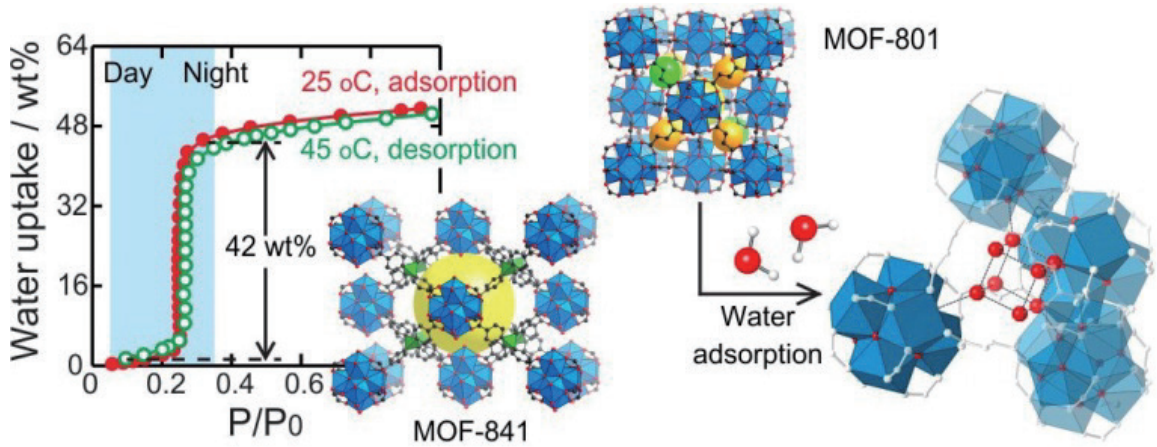

1) Pore filling or condensation of water into the pores of the solid must occur at low relative pressure (P/P_0) or relative humidity (RH), and exhibit a steep uptake behavior.
2) The high water uptake capacity for maximum delivery of water and simple adsorption/ desorption processes for energy efficiency.
3) High cycling performance and water stability of the material.

Metal-Organic Frameworks (MOFs) have been examined for their water adsorption properties. A variety of zirconium-based MOFs were designed to meet the three criteria mentioned above. Their water adsorption behaviours were examined by using a **BELSORP-aqua3** at the University of California, Berkeley.

Key words : MOF, Water adsorption, Capture and release of atmospheric water, Cycle performance

02. EXPERIMENT

Water vapor adsorption isotherms of zirconium-based MOFs and zeolite 13X at 25 °C were measured on a BELSORP-aqua3 (present model: **BELSORP MAX X HT**) volumetric vapor adsorption analyser. User-friendly measurement software enables unattended cycle performance testing over five consecutive cycles. The sample was evacuated 2 hours at 25 °C between cycles. It can also measure 3 samples simultaneously, enabling high-throughput measurements.

RESULTS AND DISCUSSION

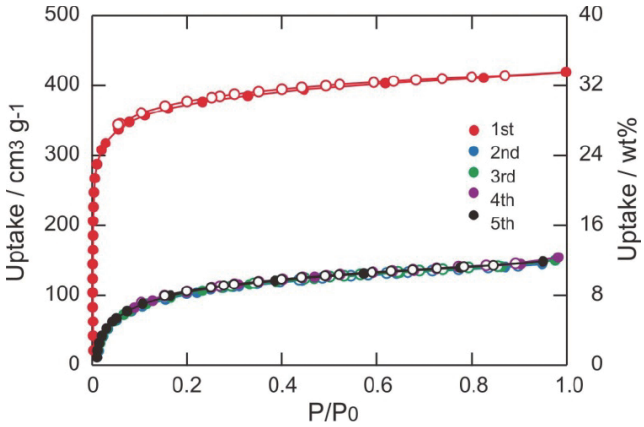

Fig.1 Cycle performance of water uptake in Zeolite 13X at 25 °C

Zeolites are commercially used to capture water in electric dehumidifiers because of their ability to adsorb water at very low relative pressures. However, due to the strong interaction between zeolites and water molecules, it is necessary to heat the material up to 300˚C to desorb the adsorbed water molecues from the pore. This regeneration process requires high energy input. Therefore, zeolites are not ideal materials for applications related to water capture and release.

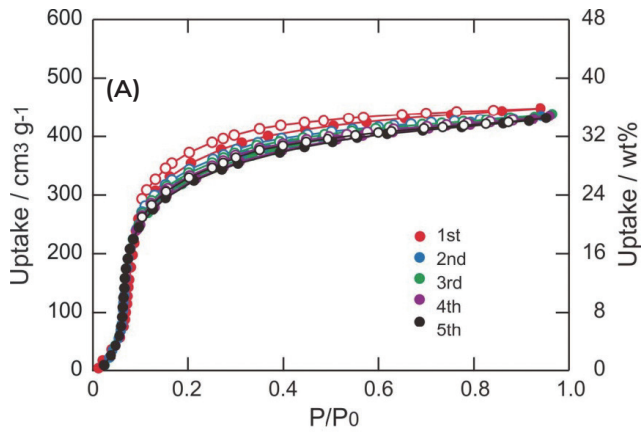

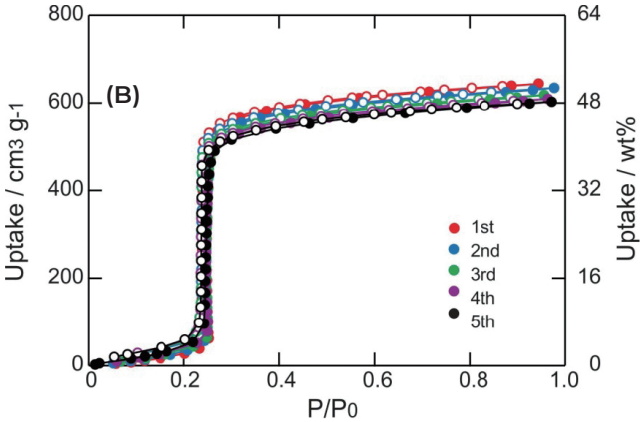

Fig.2 Cycle performance of water uptake in MOF-801-P (A) and MOF-841 (B) at 25˚C

Microcrystalline powder sample of MOF-801-P(Fig.2 (A)) and MOF-841 (Fig.2 (B)) showed high performance based on above three criteria. The water uptake in these MOF materials was steep and the maximam uptake was nearly constant even after five consecutive cycles. This clearly indicates that the these MOF materials show strong interaction with water but can be easily regenerated under mild conditions.

In order to utilzie MOFs as heat exchangers for on-board vehicles (so-called thermal batteries), water capture at low relative pressures (P/P_o < 0.1) is desirable as it reduces the need to incorporate compressors or to raise the evaporation temperature for the adsorption/desorption cycles. In that regard, MOF-801-P is a good candidate to be used in advanced thermal batteries.

MOFs can also be used for water harvesting applications to capture atmospheric water in remote desert areas. In such areas typical summer daytime temperature and relative humidity (RH) are 40 °C and 5%, which drastically changes at night to 25 °C and 35%. Under such conditions, porous materials capture water between 5% and 35% RH (i.e. P/P0 = 0.05-0.35), then water vapor in the air can be condensed. Considering that MOF-841 took up 44% of water at P/P0 = 0.3, MOF-841 has great potential to capture and release atmospheric water.

CONCLUSION

Zirconium-based MOFs demonstrate high performance for the applications requiring capture, store and release of water. Through the water vapor adsorption instrument, the uptake of water by MOFs is evaluated and their cyclability was effectively studied in this application note. However, uptake capacity and cyclic stability also depends on the defects in the crystal structure of the MOFs (2).

Reference
(1) Furukawa, H. et al. J. Am. Chem. Soc. 136, 4369–4381 (2014).
(2) Gökpinar, S. et al. Ind. Eng. Chem. Res. 58, 21493–21503 (2019).

EQUIPMENT

Gas & Vapor Adsorption Analyzer

BELSORP MAX X HT

Measurement items

- Surface area
- Pore size distribution
- Gas & vapor adsorption

SAMPLE ANALYSIS AND DEMONSTRATION

MICROTRAC accepts requests for analysis and demonstrations at any time.
Please check the measurement accuracy by sample analysis and operability by demonstration.
We are also available for consultations on measurements. Please do not hesitate to contact us.

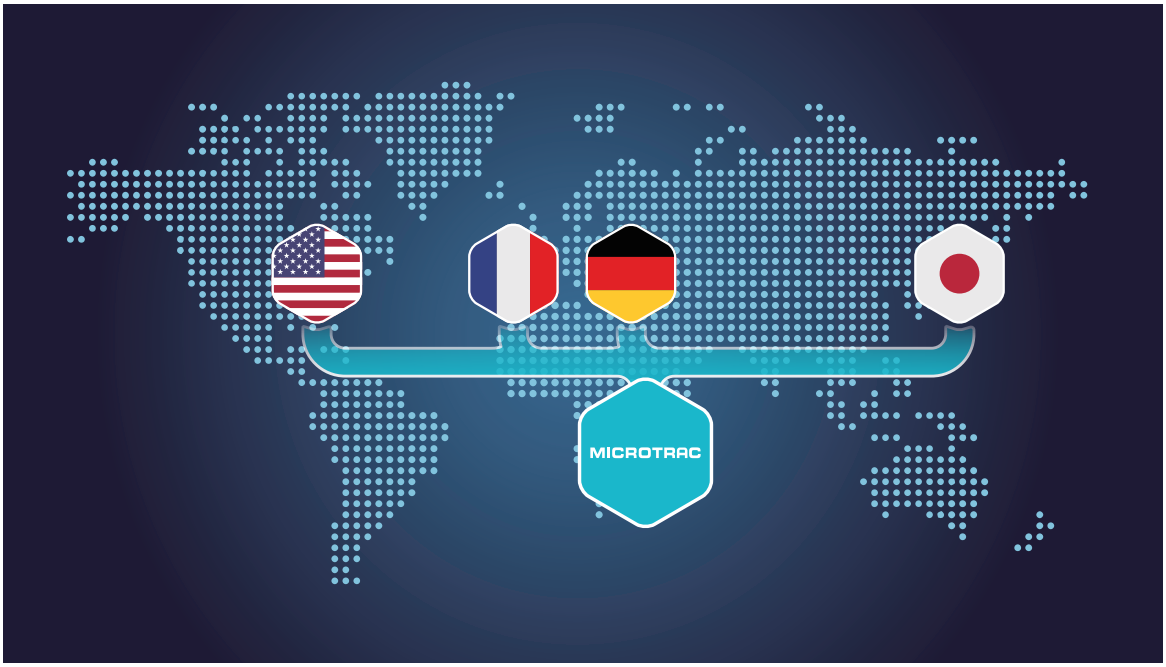

Microtrac Inc.
3230 N. Susquehanna Trail
York, PA 17406 · USA

Phone: +1 888 643 5880
marketing@microtrac.com

MicrotracBEL Corp.
8-2-52 Nanko Higashi, Suminoe-ku
Osaka 559-0031 · Japan

Phone: +81 6 6 655 0360
info@microtrac-bel.com

Microtrac Retsch Gmbh
Retsch-Allee 1-5
42781 Haan · Germany

Phone: +49 2104 2333 300
info@microtrac.com

Microtrac Formulaction SAS
3-5 rue Paule Raymondis
31200 Toulouse · France

Phone: +33 (0)5 62 89 29 29
contact.fr@mtf.verder.com

MICROTRAC
PARTICLE CHARACTERIZATION

Products (goods and services) listed in this document may fall under the category of export controlled items, etc. under the Foreign Exchange and Foreign Trade Law (Foreign Exchange and Foreign Trade Law), depending on the country of export and the intended use of the product.Export of products (goods and services) that fall under the category of restricted items must be examined by the Japanese government to obtain permission, approval, etc.

MICROTRAC
PARTICLE CHARACTERIZATION

Microtrac Inc.
3230 N. Susquehanna Trail
York, PA 17406 · USA

Phone: +1 888 643 5880
marketing@microtrac.com

MicrotracBEL Corp.
8-2-52 Nanko Higashi, Suminoe-ku
Osaka 559-0031 · Japan

Phone: +81 6 6655 0360
info@microtrac-bel.com

Microtrac Retsch GmbH
Retsch-Allee 1-5
42781 Haan · Germany

Phone: +49 2104 2333 300
info@microtrac.com

Microtrac Formulaction SAS
5 rue Paule Raymondis
31200 Toulouse · France

Phone: +33 (0)5 62 89 29 29
contact.fr@mtf.verder.com

www.microtrac.com

part of VERDER

Subject to technical changes and print errors.
Copyright © 2025 by Microtrac Retsch GmbH | 980.2042/E | 05-2025